AMRO
ASEAN +3 MACROECONOMIC RESEARCH OFFICE

Working Paper (WP/25-03)

Biodiversity Linked Bonds: An Option Pricing Based Valuation Approach

Jorge A. Chan-Lau

February 2025

[This page is intentionally left blank]

Biodiversity Linked Bonds: An Option Pricing Based Valuation Approach

Prepared by Jorge A. Chan-Lau [1]

Authorized by Laura Britt Fermo

February 2025

Abstract

Ecosystem services are essential for life on Earth and ensuring their continued provision requires the protection and restoration of biodiversity. But the scale of financing needed to protect biodiversity far exceeds the capacity of the public sector making it necessary to attract private capital. Biodiversity-linked bonds, derived from ESG sustainability-linked bonds, could help channel the required capital to biodiversity conservation as their flexible payoff structures can accommodate the preferences of both issuers and investors. This paper proposes an option-pricing based valuation framework that addresses two key characteristics of biodiversity-linked bonds: first, the optionality embedded in the bond's payoff structure, and second, the constraints on the family of stochastic processes suitable for modeling complex biodiversity dynamics. A standardized pricing framework could support scaling up biodiversity markets and help to narrow the existing funding gap.

JEL classification: Q51, Q57, G32

Keywords: Biodiversity, contingent claims, option pricing, sustainability linked bonds, stochastic differential equations.

[1] Author's e-mails: jchanlau@gmail.com (permanent) and Jorge.Chan-Lau@amro-asia.org. I thank Ralph Chami for introducing me to this topic , Thomas Cosimano and Roger Iles for stimulating discussions on the valuation of nature, and Laura Britt Fermo, Michael Wynn, seminar participants at AMRO, and colleagues at the Central Bank and the Department of Finance of the Philippines for useful comments. I am solely responsible for any errors and omissions.

Contents

List of Figures

List of Tables

1 Introduction

Ecosystems provide valuable services complementary to other production factors and make life possible on Earth. In 2020, approximately US$ 44 trillion of global GDP was dependent on ecosystem services (Herweijer et al. 2020). The services fall under four main categories (Millenium Ecosystem Assessment 2005):

- Provisioning services, which are the tangible goods and resources that humans can harvest from the system. They comprise food, water, raw materials, genetic resources, and medicines.
- Regulating services, which are the benefits ecosystems provide by stabilizing the environment. Key among them are climate regulation, water regulation, air purification, pest and disease control, and pollination.
- Cultural services, which are benefits that contribute to society's quality of life, cultural identity, and well-being more generally. They include, among others, recreation, aesthetic value, spiritual and religious significance, education, and social cohesion.
- Supporting services which are essential to the overall health and function of the ecosystem, and sustain the three other type of services. Some of them include soil formation, nutrient and water cycling, and biodiversity.

The ecosystem biodiversity is a critical factor in the provisioning of services and should be preserved as much as possible, as the services ecosystems provide cannot be substituted away by increasing the stock of human-created physical capital (Dasgupta 2021).[1]. Biodiversity is not uniformly distributed in the planet but largely concentrated in the tropical and subtropical regions. The most biodiverse areas include the tropical rainforests in Africa, South America, and Southeast Asia; the coral reefs in Australia, the Caribbean, and Southeast Asia; the tropical Andean regions in Colombia, Ecuador, and Peru; and the mangrove forests in Central and South America, Southeast Asia, and West Africa (Hoekstra et al. 2010).

A majority of the most biodiverse countries are either developing or emerging market economies, where nature represents a substantial share of their wealth (Figure 1). This is partly because they have not accumulated as much human and non-natural physical capital as in several advanced economies, and because deforestation and over-exploitation of natural resources have yet to reach the levels experienced by the latter earlier during their development stage. Nevertheless, these ecosystems are increasingly under duress (Conservation International 2024).

1. Ecosystem services can be formally integrated into a production function to evaluate the overall impact of biodiversity loss in the economy and assess how fragine an ecosystem is, as in Giglio et al. (2024)

Figure 1. Share of renewable natural capital in total wealth vs. 2022 PPP GDP

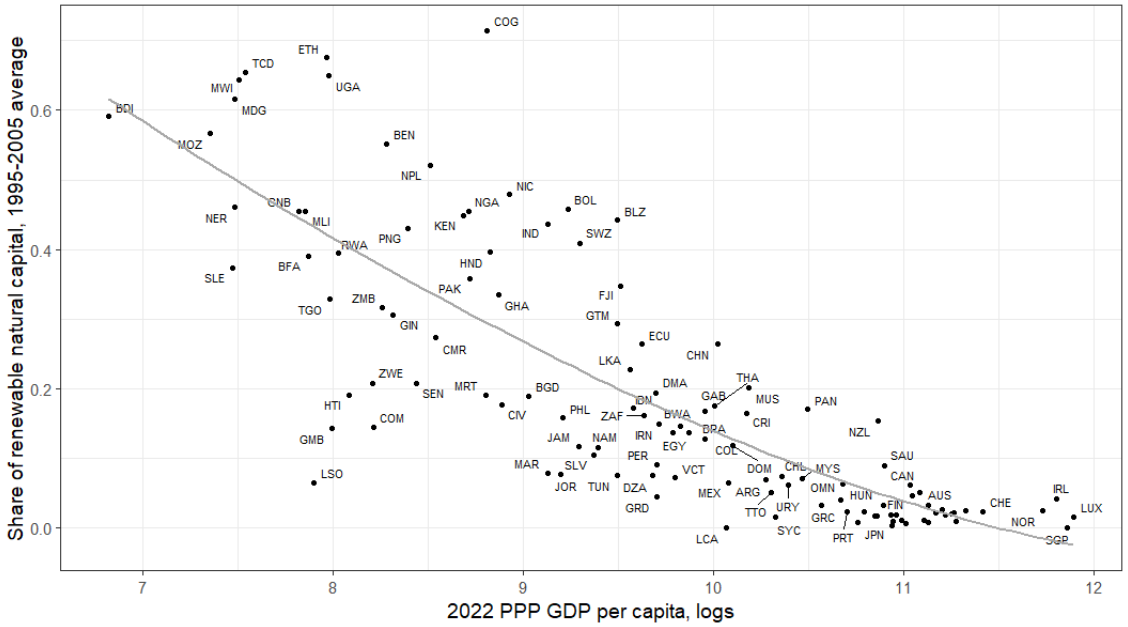

Sources: Notre Dame Global Adaptation Initiative (ND-GAIN), and the World Bank.
Notes: The figure shows the ND-GAIN ID ECOS 03 index against the 2022 PPP GDP World Bank estimates. The index is based on the World Bank's Natural Capital Accounting Project and is an indicator of the strength of the dependency of social systems on ecosystems goods and services. It is based on the deployment of national capital in national accounting including national income and savings in the form of all assets and capital goods that are inputs to economic well-being (World Bank 2010). The natural capital related to ecosystem services includes: crop, pasture, forest (timber), forest (non-timber) and protected areas. Sub-surface capital such as oil, gas and mineral reserves are not included.

Limited financial resources, combined with the urgent demands of growing populations, make it difficult for developing and emerging economies to prioritize environmental protection in the same way that advanced economies can. Wealthier economies have more robust institutions and access to funding for sustainability initiatives, as evident in Figure 2. The disparity underscores the need for more equitable global support and innovative financing mechanisms to finance environmental protection efforts. But mobilizing the needed resources to protect biodiversity is a Herculean task. Deutz et al. (2020) suggest that from 2020 until 2030, global biodiversity conservation needs would require annual outlays of between US$ 680 billion to US$ 950 billion, which vastly exceeds conservation funding annual flows of only between US$ 118 billion to US$ 154 billion. The needs are associated with the expansion of protected areas, the conservation and restoration of coastal ecosystems, the sustainable management of productive landscapes and seascapes, the management of invasive species, the biodiversity conservation in urban environments and the reduction of water pollution.

Figure 2. Enviromental Protection Index Score vs. 2022 PPP GDP

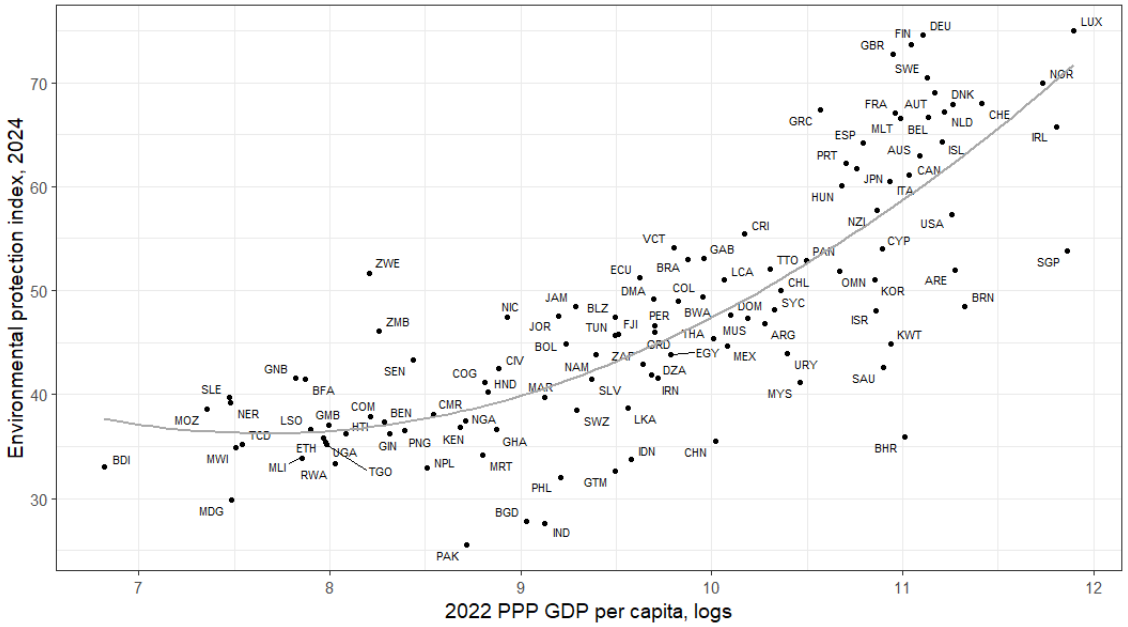

Sources: Yale Center for Environmental Law and Policy, and the World Bank.
Notes: The EPI score is a data-driven summary of the state of sustainabilty based on 58 performance indicators across 11 environmental issues including climate change mitigation, air quality, sanitation and drinking water, heavy metals, solid waste, water resources, agriculture, fisheries, air pollution, forests, and biodiversity and habitat (Block et al. 2024).

A number of reasons suggest public funds alone will be insufficient to close the biodiversity funding gap. Among them, one is the enormous scale of biodiversity conservation, as highlighted earlier. A second one is that governments must attend to competing priorities among which biodiversity would likely rank among the least urgent. The problem is compounded by the political cycle which diverts policymakers' attention from long-term issues such as biodiversity and climate finance. Finally, most of the rich biodiversity areas are located in developing countries with limited scope for spending resources in biodiversity conservation. The benefits of biodiversity conservation, however, are shared worldwide, which strongly supports the North-South mobilization of funds for that purpose. However, the failure to mobilize funds to address climate change suggests serious headwinds for global cooperation in biodiversity conservation and the associated fund transfers (United Nations Framework Convention on Climate Change 2022). To bridge this gap, there is a growing call for increasing private sector engagement, especially by attracting institutional and high net worth investors interested in wealth preservation and enhanced financial returns.[2]

Innovative financial instruments could help to scale up conservation projects by providing investors with the investment opportunities they are seeking for and fostering the

2. For instance, the ASEAN biodiversity plan calls for an annual mobilization of US$ 200 billion per year, inciuding US$ 30 billion through private sector funding (ASEAN Centre for Biodiversity 2023).

creation of a new asset class.[3] One such instrument is the sustainability linked bond (SLBs) (Erlandsson et al. 2024). The bond's payoff, either coupons and/or principal repayment, are contingent on whether certain sustainability indicators meet predefined targets or objectives. The bond issuer, by taking certain actions and measures, can increase the likelihood of achieving the objectives. The objectives are measured using key performance indicators (KPI) which are verified by a third party not involved in the transaction. The bonds, which generally follow the principles proposed by the ICMA (2024), have been issued mainly by corporations aiming at net zero targets and could be instrumental in achieving them (Murphy 2022). The advantages SLBs confer do not need to be confined to corporate issuers though, as they could also help sovereign countries to achieve their green targets by tapping into private funding sources, as Chile and Uruguay did in 2022 (Cheng, Ehlers, and Packer 2022, Padin-Dujon and Filewood 2023).

The rapid growth of the market of SLBs targeting net zero emissions suggests it is promising to develop similar biodiversity-linked bonds (BLBs). Although net zero SLBs' share in the global sustainable debt market remains small at 2 percent of the total market volume, this market segment has almost doubled in 2023 (Chouhan, Harrison, and Sharma 2024). Some of the growth might have been driven by one attractive feature of these bonds: they only require the issuer to improve its sustainabilty performance, and contrary to green bonds, there are no limitations on the use of the bond's proceeds.[4] Introducing SLBs linked to biodiversity targets, such as habitat restoration or species protection, could leverage this momentum and help bridge the biodiversity funding gap, addressing the concerns expressed in Karolyi and Tobin-de la Puente (2023).[5]

Besides easier target monitoring, the flexible payment structure of a BLB, which accommodates the needs of issuers and investors, could facilitate its widespread use in biodiversity conservation. The payment structure of the 5-year Wildlife Conservation Fund (a.k.a. Rhino Bond) issued by the World Bank in March 2022 illustrates this flexibility. The cash flows from investing the bond principal are used to fund rhino conservation efforts. The investor in the Rhino Bond will redeem its principal and receive a conservation success payment contingent on the rhino population growth observed at the contract maturity.To reduce risks to the investor, the contract is guaranteed by the World Bank and the Global Environment Facility, which serves to reduce the risks to the investor (World Bank 2022, Medina and Scales 2024).

This paper contributes to the literature on biodiversity financing by proposing a

3. Credit Suisse, World Wildlife Fund, and McKinsey Center for Business and Environment (2014) and (Credit Suisse and McKinsey Center for Business and Environment 2016).

4. As any other financial instrument, SLBs are not perfect instruments. Their shortcomings are not reviewed here but the interested reader is referred to Haq and Doumbia (2022) for a more extensive discussion. Medina and Scales (2024), argue that using financial instruments for funding biodiversity may give investors excessive influence on key decisions.

5. Notwithstanding the importance of privatee capital, they cannot be a substitute for effective public policies (Flammer, Giroux, and Heal 2025). Equally important, as in green finance and ESG initiatives, efforts should be made to reduce the risk of greenwashing (Maron, Martine et al. 2023).

benchmark valuation approach for BLBs. Since they constitute a special case of the more general SLBs, the option pricing approach developed for the latter can be extended to BLBs. The benchmark valuation approach, however, should be adapted to accommodate two key characteristics of biodiversity assets that differentiate BLBs from other SLBs. First, an ecosystem's ability to support biodiversity — measured through metrics such as an index, species count, or the population size of specific species — is limited by the ecosystem's carrying capacity, as basic life-sustaining resources are finite, and species compete for them. Second, when biodiversity falls below a critical threshold known as the Allee threshold, the ecosystem may lose its capacity for regeneration, leading to species extinction.[6] Additionally, the framework accounts for human activities — commonly referred to as the "economic program" (Fenichel and Abbott 2014) — which influence biodiversity dynamics through their direct and indirect environmental impacts.

The core principle of the proposed valuation approach is the integration of existing biological and ecological stochastic models of biodiversity growth into a standard option pricing framework. This final component is necessary to capture the optionality embedded in the payoff structure of BLBs. To illustrate the approach, several simple BLB instruments — which can serve as building blocks for more complex structured notes — are priced using realistic parameters derived from empirical studies. Hence, this paper addresses the call for further research into nature financing, as urged by Karolyi and Tobin-de la Puente (2023), while providing practitioners with a useful and implementable framework for evaluating the risk-return profiles of BLBs.

The remainder of the paper proceeds as follows: section 2 reviews the relevant literature, laying the foundation for the subsequent analysis. Section 3 introduces the pricing method, explaining its key features and underlying principles, and section 4 illustrates its application with an example based on fisheries' data. Finally, section 5 concludes with a discussion of the broader implications and potential future directions for research.

2 Literature Review

SLBs have been issued using a variety of formats including plain vanilla SLBs, hybrid SLBs, and convertible SLBs. The most common format, however, is the plain vanilla SLB (Erlandsson et al. 2024). This instrument is a standard fixed income bond that pays either fixed or floating rate coupons. The bonds are bundled with an option-like step-up or step-down coupon structure. The step-up coupon structure becomes active, or in option pricing parlance, becomes in-the-money (ITM) when a KPI or a set of KPIs fail to meet pre-defined sustainability performance targets (SPTs) during the life of the bond. In the case of a step-down coupon structure, it becomes ITM when the SPTs are met.

An option pricing framework is appropriate to value SLBs because of their option-

6. See Taylor and Weder (2023) for an analysis of extinction economics and case studies, and the less technical overview in Taylor and Weder (2024).

like step coupon structure, as done in earlier studies.[7] Outside biodiversity, a unified framework or benchmark model has yet to emerge due the complexity of modeling the dynamics of the ESG-related key performance indicators (KPI). There are no universally accepted standards or taxonomies for ESG metrics, which drives discrepancies in the definition and measurement of ESG sustainability targets. Although useful voluntary guidelines have been issued (ICMA 2024) they are subject to a wide interpretation. The absence of ESG standardization and the high degree of subjectivity involved in their choice and measurement is reflected in the ample dispersion of ESG ratings (Berg, Koelbel, and Rigobon 2022) and raises concerns about greenwashing problems, which seems apparent in the data (Du, Harford, and Shin 2024, Lam and Wurgler 2024).

Several additional factors further complicate establishing a benchmark option pricing model for ESG-related SLBs. One is that many KPIs cannot be quantified explicitly. For instance, they include discrete choice events such as the introduction of ESG-related corporate governance principles, i.e. diversity representation in the board of directors. A second factor is that the payment structure in several ESG SLBs depends on meeting several KPIs targets. The valuation problem becomes a multi-asset option pricing problem and requires modeling the comovements of the KPIs. This is not an easy task in the absence of quality data on potentially ill-defined metrics (Mielnik and Erlandsson 2022). A third factor is that ESG SLBs are typically issued by firms, and the default risk associated with these issuers may not be negligible. The credit risk of the firm must be integrated into the model since the firm's default compromises its ability to meet both its financial obligations, including the SLBs it has issued.

Despite these challenges, there is a growing literature on the use of option pricing to value ESG-related SLBs. Among them, Mielnik and Erlandsson (2022) and Erlandsson et al. (2024) are the studies closest to this paper's approach. Both studies focus on SLBs with a step-up coupon option. They note that this structure is equivalent to a traditional fixed rate bond paying the normal coupon bundled with a binary option, the step-up coupon. The latter is a binary option since it is in-the-money only when the issuer fails to meet the ESG target. Mielnik and Erlandsson (2022) illustrate the option pricing approach by valuing two corporate SLBs, one of them linked to an observable KPI, the emissions' intensity relative to output produced, and the other linked to an unobservable, non-priced KPI. In the latter case, a proxy KPI is used. Erlandsson et al. (2024) extend the analysis of the previous study by examining numerous case studies, analyzing structures other than plain vanilla SLBs, and evaluating the role of SLBs in fixed income portfolios. Section 3 in this paper extends and specializes their approach to BLBs, where the dynamics of the sustainability indicators, which are constrained by the laws of nature, are incorporated explicitly in the option pricing framework.

As in Mielnik and Erlandsson (2022), Feldhutter, Halskov, and Krebbers (2024) show,

7. See Erlandsson et al. 2024 and references therein.

within a default risk intensity model framework, that the price of SLB can be decomposed into two components, : a "sustanium" bond without any option-linked cash flows and option-linked cash flows associated with the ESG targets. They are able to extract the ESG premium for a SLB after calibrating their model by extracting the bond issuer's default hazard rate from the prices of its ordinary (non-ESG) bonds; computing the sustanium, or the risk premium investors are willing to pay for an option-free sustainability bond, from a subset of SLBs without option-linked cash flows; and estimating the expected value of the option-linked cash flows assuming that the observable KPIs follow a geometric Brownian motion. Their results suggest that ESG SLBs are priced at slightly higher prices than non-ESG bonds. They also find that among the firms in their data sample, targets are easy to reach as the average probability of missing them was only from 14 percent to 39 percent.

The finding that many firms set low sustainability targets raises concerns about greenwashing as issuers may seek to benefit from lower yields without a serious commitment to sustainability efforts (de Mariz et al. 2024, Erlandsson et al. 2024). However, simply setting higher targets may not effectively mitigate greenwashing risk. The financial rewards of issuing a SLB often outweigh the penalties incurred if targets are not met (Kolbel and Lambillon 2023). Additionally, markets tend to reward issuers with lower yields as targets become more ambitious, a practice that may not be fully justified. Specifically, Chen, Hinken, and Loffler (2024) argue that model-based fair price yields do not necessarily have to increase as targets become more demanding. Consequently, market practices may grant issuers of SLBs that set high and more unlikely targets a wider spread between the bond's yield and the penalty for missing the target, compared to issuers who set more realistic, lower targets.

This section ends by highlighting that the payoff structure of a plain vanilla SLB is similar to that of a social impact bond (SIB). The latter targets social goals such as reducing recividism. In this case, the proceeds of the SIB, typically issued by local governments, are used to achieve the social goal target. Coupons step-up if the target is not met. Andrikopoulos and Tsekrekos (2024) suggest that SIBs could be valued as real options since they are equivalent to a non-traded European put spread option on a non-traded asset. If the non-traded assets is correlated with a traded asset, they suggest pricing the SIB using the incomplete market option pricing framework of Davis (1999). This approach, however, might not be feasible for BLBs and SLBs, as it is likely that biodiversity and ESG correlated traded assets are not available.

3 Biodiversity-linked bonds: basic pricing framework and principles

BLBs are SLBs with biodiversity KPIs (population growth, biodiversity indicators, etc.) whose dynamics are constrained by two key characteristics of an ecosystem, its carrying capacity and the Allee effect. The first characteristic places an upper bound on the

biodiversity level of the ecosystem. The second characteristic implies that, below a certain level, the ecosystem and its biodiversity become extinct. Pricing a BLB requires pricing the step coupons using an option pricing framework in which the underlying, the KPI, follows a stochastic process that can accommodate the ecosystem carrying capacity and the Allee effect. Closed form solutions might not be available but numerical methods can be used once the process is calibrated using parameters from empirical studies. After describing in more detail what the carrying capacity and Allee effect are, this section describes several benchmark stochastic processes useful for pricing BLBs. Numerical methods are then used to price simple BLB contracts linked to the population dynamics of the Pacific halibut using the parameters estimated by Hanson and Ryan (1998) and reported in Braumann (2019).

3.1 Carrying capacity and Allee effect

Most biodiversity performance indicators are inherently limited by the ecological concept of carrying capacity, which refers to the maximum number of individuals, species, or functions that an ecosystem can sustainably support. This capacity is influenced by various factors, including resource availability, habitat size, environmental conditions, and species interactions. As ecosystems reach their carrying capacity, any further increase in population can lead to competition for resources, habitat degradation, and ultimately, a decline in biodiversity.

Equally important, any pricing model should account for the Allee effect. When biodiversity falls below a critical threshold, the Allee threshold, the ecosystem may struggle to recover and may collapse over time (Allee 1931). The Allee effect occurs because at very low biodiversity levels, the resilience of the ecosystem is reduced and its ability to withstand environmental stresses and maintain essential functions is fatally impaired. As a result, instead of stabilizing or recovering, the ecosystem biodiversity deteriorates continuously until the ecosystem is destroyed.

In ecosystems, the carrying capacity and the Allee effect impose limitations on the types of stochastic processes that should be used when pricing the contingent payment structures embedded in BLBs. Stochastic processes that allow carrying capacity and the Allee effect to influence the biodiversity dynamics include the stochastic logistic growth model (Levins 1969,Capocelli and Ricciardi 1974) extended to include the Allee effect (Jiang, Shi, and Zhao 2005, Krstic and Jovanovic 2010 and Carlos and Braumann 2017), its generalized version (Saha et al. 2013, Sau, Saha, and Bhattacharya 2020), and the stochastic Gompertz growth model with Allee effect (Amarti et al. 2018). For pricing BLBs, it is convenient to use numerical methods, especially if the stochastic growth models are augmented by a human utilization term. Exact solutions, however, are available for some special cases (Skiadas 2010, Brites 2017)

3.2 Stochastic growth models with carrying capacity and Allee effects

There are several stochastic processes that can accommodate the carrying capacity and Allee effects. The most widely used is the ***stochastic logistic growth model with Allee effects***. In this model, the rate of change at time t, dX, of the biodiversity stock, X_t, for any period $t \in [0, T_f]$, follows the stochastic differential equation (SDE) below:

$$dX_t = \left(rX_t \left(1 - \frac{X_t}{K} \right) \left(\frac{X_t}{E} - 1 \right) - \theta X_t \right) dt + \sigma X_t dW_t, \quad t \in [0, T_f], \tag{1}$$

where r is the intrinsic growth rate of the population (or biodiversity indicator) which would be observed in the absence of carrying capacity and Allee effects and random shocks, and σ is the diffusion coefficient that magnifies the random shocks, which are modeled as a W_t a standard Wiener process.[8]

The drift coefficient in equation (1) is equal to the product of the instantaneous growth rate, r, the capacity carrying term, $(1 - X_t/K)$, and the Allee effect term, $(X_t/E - 1)$ net of the reduction in biodiversity due to human action, θX_t, which is assumed has a negative linear effect on the biodiversity stock. When framed within the context of biodiversity conservation, human action can be mitigated or reduced to bolster the growth rate of the population. The capacity carrying threshold, K, is the level above which the rate of change of the biodiversity stock becomes negative as the ecosystem is unable to generate the needed resources to sustain positive biodiversity growth. The Allee threshold, E, is the level below which the biodiversity stock becomes too small to be able to regenerate itself. Once the threshold is crossed from above, growth becomes negative and leads to the demise of the ecosystem and its biodiversity. The introduction of the Allee effect forces the growth rate to be asymmetric on both sides of the midpoint $X = K/2$, in sharp contrast to its counterpart without Allee effect.

In the ***generalized logistic growth process with Allee effects*** the SDE determining the growth rate of the biodiversity stock is:

$$dX_t = \left(rX_t \left(1 - \left(\frac{X_t}{K} \right)^{\alpha} \right) \left(\frac{X_t}{E} - 1 \right) - \theta X_t \right) dt + \sigma X_t dW_t, \quad t \in [0, T_f], \tag{2}$$

where the parameter $\alpha > 0$ allows it to model a broader range of growth behavior compared to the standard stochastic logistic growth model. When $\alpha = 1$, the model reduces to its standard version. When $\alpha > 1$, the growth curve has a sharper transition to the carrying capacity threshold. If $\alpha < 1$, the transition is more gradual. All the other parameters are the same as in the standard logistic growth model of equation (1).

8. See Oksendal (2013) for a comprehensive treatment of stochastic differential equations and Braumann (2019) for applications in biology.

In ecosystems where biodiversity first experiences an initial slow growth phase and exponential decay in the growth rate afterwards, the preferred model is the ***stochastic Gompertz growth model with Allee effect***. Its SDE is:

$$dX_t = \left(rX_t \log\left(\frac{K}{X_t}\right) \log\left(\frac{X_t}{E}\right) - \theta X_t \right) dt + \sigma X_t dW_t, \quad t \in [0, T_f], \tag{3}$$

where all the parameters are defined as in equation (1).

To compare different the embedded optionality of SLBs, it is convenient to express time as a fraction of the length of the time horizon, i.e. $\tau = t/T_f$, and the biodiversity stock and Allee threshold as fractions of the carrying capacity, $Y_t = X_t/K$ and $E_K = E/K$ respectively. The normalization rescales the time horizon to $[0, 1]$ and the carrying capacity to 1. Equation (1) is now equivalent to the normalized stochastic logistic growth model with Allee effect:

$$dY_\tau = \left(r^* Y_\tau \left(1 - Y_\tau\right) \left(\frac{Y_\tau}{E_K} - 1\right) - \theta^* Y_\tau \right) d\tau + \sigma^* Y_\tau dW_\tau, \quad \tau \in [0, 1], \tag{4}$$

where $r^* = rT_f$, $\theta^* = \theta T_f$ and $\sigma^* = \sigma\sqrt{T_f}$. Equation (1) does not have a closed form solution but given the parameters $(r^*, \theta, \sigma^*, E_K)$, or the original set of parameters necessary to derive them, $(r, \theta, K, E, \sigma, T_f)$, it can be solved numerically (Kloeden and Platen 1999). Note also that the numerical solutions of either equation (1) or equation (2) yields the physical or real world probabilities that the value of the biodiversity stock (or indicator) exceeds or falls short of reaching a certain pre-specified value. Similarly, the normalized SDE of the generalized logistic growth model with Allee effect is:

$$dY_\tau = \left(r^* Y_\tau \left(1 - Y_\tau^\alpha\right) \left(\frac{Y_\tau}{E_K} - 1\right) - \theta^* Y_\tau \right) d\tau + \sigma^* Y_\tau dW_\tau, \quad \tau \in [0, 1], \tag{5}$$

and the normalized SDE of the stochastic Gompertz growth model with Allee effect is:

$$dY_\tau = \left(-r^* Y_\tau \log\left(Y_\tau\right) \log\left(\frac{Y_\tau}{E_k}\right) - \theta^* Y_\tau \right) d\tau + \sigma^* Y_\tau dW_\tau, \quad \tau \in [0, 1]. \tag{6}$$

Equations (1) to (3) and their normalized forms are specific examples of SDEs that account for both carrying capacity and Allee effects. Alternative functional forms can also be applied, as highlighted in the references discussed in the literature review. What matters the most is that the choice of the functional form should align with the characteristics of the biodiversity data.

3.3 Computation of the BLB's premium

Computing the BLB premium is contract specific, as it requires specifying the BLB's cash flows, the risk aversion of the investor, and whether the issuer might default or not. More

likely than not, the pricing of the BLB and the computation of its premium requires using numerical methods, as in the binary BLB coupon option example analzyed later in the paper. However, there are some basic principles for setting up the option framework that apply to all contracts, mainly due to the existence of the Allee effect.

Like any other SLB, the BLB is a standard bond combined with an additional option-like coupon. To value this option-like coupon, the analysis assumes that the dynamics of the biodiversity KPI (BKPI) follow the stochastic processes described earlier, with better outcomes reflected in higher BKPI values. The coupon can be structured as either a step-down or step-up option. These step coupon payoffs are path-dependent, contingent on the BKPI's performance over the lifetime of the BLB. Payoffs may be delivered at expiration (European-style) or triggered immediately when the BKPI reaches the step coupon threshold (American-style). Real-world examples suggest that issuers and investors often prefer American-style step coupons (Erlandsson et al. 2024).

In the case of a step-down, the issuer benefits from reduced coupon payments once the BKPI reaches pre-specified biodiversity performance target (BPT). This assumes that the initial value of the BKPI at contract inception is lower than the BPT. The BKPI performance could be monitored continuously or at discrete times throughout the life of the BSLB. More complex payoffs are also possible. For example, the coupon reduction could be contingent on the BKPI remaining at or above the BPT for the remainder of the BLB's life after first reaching it. Alternatively, the coupon reduction could be proportional to the fraction of the BLB's life during which the BKPI stays at or above the BPT.

The presence of the Allee effect makes step-down coupon structures resemble down-and-out barrier options. When the BKPI reaches or falls below the Allee threshold for the first time, the likelihood of ecosystem collapse significantly increases. At this point, the step-down coupon becomes worthless, regardless of whether the option is European or American style. This assumes that investors treat hitting the Allee threshold as a failure event. However, given the stochastic nature of BKPI dynamics, there remains a possibility that a series of positive shocks could enable the BKPI to recover and rise above the threshold.

When the bundled option is a step-up coupon, the issuer of the BLB benefits from a lower coupon rate compared to a similar standard bond without the step-up feature. Assuming the initial value of the BKPI is lower than the BPT, the step-up coupon is activated the first time that the BKPI fails to reach the BPT after an initial grace period under continuous monitoring. As an alternative, several discrete observation times could be agreed at contract inception time, with the step-up coupon triggered at the first instance of the observation time when the BKPI fails to reach the BPT. If the value of the BKPI at the contract's inception is above the BPT, the step-up coupon is triggered the moment the BKPI falls below the BPT, either immediately under continuous monitoring, or at the first observation time when this event occurs under monitoring only at discrete times. It

is worth noting that the Allee effects adds a down-and-in feature to the step-up coupon regardless of the initial BKPI value or whether the option is European-style or American style. Once the BKPI reaches the Allee threshold, the coupon is triggered.

4 A binary BLB step-down coupon option example

Let's consider a BLB that pays a single coupon C at maturity and includes a step-down coupon option, or a binary BLB coupon option. Assume the investor is risk-neutral, and the issuer is default risk-free. A standard bond without the step-down coupon would pay a coupon equal to the cumulative risk-free rate earned over the bond's life. Because of risk-neutrality, the risk-free rate should also be the expected return the investor receives from the BLB. Therefore, the bond should be issued with a higher maturity coupon, C_0, since there is a positive probability that the step-down option is triggered, thereby reducing the coupon paid at maturity. Suppose that the step-down coupon is a fraction, δ, of the cumulative risk-free rate, R_f, and that the probability that the BKPI hits the BPT, the in-the-money probability, is P. The initial value of the coupon, C_0 should satisfy:

$$C_0 = (1 + \delta P)\, R_f > R_f, \quad 0 \leq P < 1. \tag{7}$$

In equation (7), the discount rate is the risk-free rate since, with certainty, the issuer will not default. If default is a non-negligible event, it would be enough to replace R_f with the risky discount rate, R_p, which accounts for the issuer's default risk. When $P = 0$, the step-down coupon will not be triggered at all and the initial coupon should be set equal to the risk-free rate, due to our assumption that the investor is risk-neutral. When $P = 1$, the coupon should be set equal to the sum of the risk-free rate and the step-down coupon, since it will always be trigerred. In both cases, the issuer will pay the risk-free rate. The probability, P, can be calculated using Monte Carlo simulation of the SDE governing the dynamics of the BKPI. In contrast to financial options, which are priced assuming a risk-neutral probability measure, the simulation of the SDEs equations using any of the equations from (1) to (6) yields physical, i.e. real world probabilities.

To price the BLB coupon option, the BKPI, X, is set equal to the stock of the Pacific Halibut, which is assumed to evolve according to equation (1). Two of the parameters are obtained from Hanson and Ryan (1998), the instanenous rate $r = 0.71/\text{year}$, and the carrying capacity $K = 8.05 \times 10^4$ tonnes. The intrinsic volatility parameter $\sigma = 0.2/\sqrt{\text{year}}$ is obtained from Braumann (2019). For the other parameters, I assume the following default values: an Allee threshold, $E = 0.15K$; an initial value of the BKPI, $X_0 = 0.3K$; a utilization rate, $\theta = 0.5r$; and a BPT, $BPT = 0.5K$. The time period for the simulation is set to $T_f = 50$ years. The Monte Carlo simulation is performed using equation (4), the normalized version of equation (1). It consists of 10,000 replications and a 1000 point discretization of the time interval $[0, 1]$. The discrete approximation of the SDE uses the Milstein method, which tends to produce better results when the diffusion coefficient

depends on the state variable Y_τ (Kloeden and Platen 1999). Due to the normalization, in the simulation results the Allee threshold and the BPT are now expressed as a fraction of K, and the times are expressed as a fraction of T_f.

Figure 3 shows the ITM probability of the step-down option being triggered in the BLB coupon bond for several combinations of the Allee threshold and the BPT while keeping all the other parameter values fixed at their default values. For a given Allee threshold value, the ITM probability remains mostly unchanged when the BPTs are increased from 40 percent to 80 percent of the carrying capacity. For the default value of 0.15, the ITM probabilty fluctuates between 0.84 to 0.85, depending on the BPT.

Figure 3. In-the-money (ITM) probability, BLB step-down coupon: biodiversity performance target sensitivity

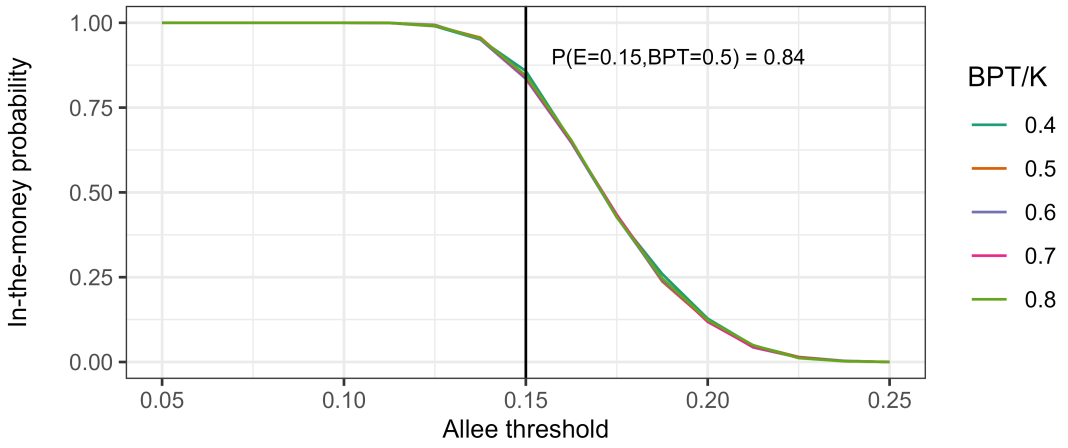

Sources: Hanson and Ryan (1998), Braumann (2019), and the author.
Notes: The figure shows the in-the-money (ITM) probability, or the probability that the step-down coupon will be triggered for different combinations of the Allee threshold and the biodiversity performance target (BPT), each reported as a fraction of the carrying capacity of the Pacific Halibut ecosystem. The Monte Carlo simulation assumes fixed values of $r^* = r \times T_f = 35.5$, $\sigma^* = r \times \sqrt{T_f} = 1.4$, $\theta^* = \theta \times T_f = 17.75$, $Y_0 = 0.30$, and 10000 replications of equation (4) using the Milstein solution scheme with a 1000 point discretization of the time interval $[0, 1]$.

Probabilities start declining rapidly as the Allee threshold increases. For instance, when the Allee threshold increases to 20 percent of the carrying capacity from the default value of 15 percent, the ITM probability falls sharply to around 12 percent, as the initial buffer of 15 percent, which is the surpluses of the initial value of the Halibut stock over the Allee threshold, falls to 10 percent. On the other hand, at lower levels of the Allee threshold, the probability of triggering the step-down coupon converges to 1 as a wider buffer offsets the variability of the Halibut stock.

When the ITM probabilities are substituted into equation (7), they generate the initial coupon values for various step-up coupons, ranging from 10 percent to 50 percent of the risk-free rate, R_f (Figure 4). The shape of the initial coupon value curves closely mirrors that of the ITM probability curves. As the ITM probabilities,the coupon values show limited sensitivity to changes in the BPT. Under the default parameter settings,

the initial coupon value is expected to be 9 percent above R_f for a step-up coupon of 10 percent of R_f, increasing to 40 percent for a step-up coupon of 50 percent of R_f. As the Allee threshold increases, it becomes more likely that the step-down coupon will not be exercised, which drives the initial coupon to converge to the risk-free interest rate. For smaller Allee thresholds, the coupon converges to the step-down coupon since it will be exercised almost certainly.

The ITM probability exhibits high sensitivity to the species' growth rate, in a sharp contrast to its sensitivity to the BPT. Figure 5 shows the ITM probability corresponding to different values of the growth rate, which is allowed to vary from $0.5r^*$ to $1.5r^*$, where $r^* = 35.5$ is the default growth rate of the Halibut populaton. As expected, for any given Allee threshold the ITM probability increases with the growth rate. Differences in growth rate lead to a wide difference in ITM probabilities for Allee threshold values in the $[0.15, 0.20]$ range. For instance, at the default Allee threshold of 0.15 the ITM probability increases to 0.99 from 0.84 when the growth rate is 50 percent higher than the default value. Were the growth rate to fall by 25 percent to $0.75r^*$, the ITM probability would decline to 0.48, almost half of the default value.

Similarly, human utilization of the natural resource have as large an impact on the IMT probability as the intrinsic growth rate (Figure 6). This is expected, as higher utilization rates reduce the drift rate governing the rate of change of the biodiversity indicator, making more difficult to reach the BPT and making more likely to hit the Allee threshold. Since the numerical analysis is based on the simulation of equation (4), a faster growth rate leads to a higher biodiversity level, Y_τ, which in turn, drives up the overall volatility of the growth process due to the diffusion coefficient, $\sigma^* Y_\tau$.

Increased volatility does not necessarily impair the ability of the biodiversity indicator to reach the BPT successfully due to the embedded optionality of the step-down coupon, as depicted in Figure 7. At low Allee threshold values, the initial size of the halibut population creates a substantial buffer above the extinction level. However, if volatility is high, negative shocks large enough to drive the ecosystem below the Allee threshold become more likely, which drives the ITM probability down while large positive shocks only have a limited impact due to the subs-

Figure 4. Initial coupon value, BLB step-down coupon: biodiversity performance target sensitivity

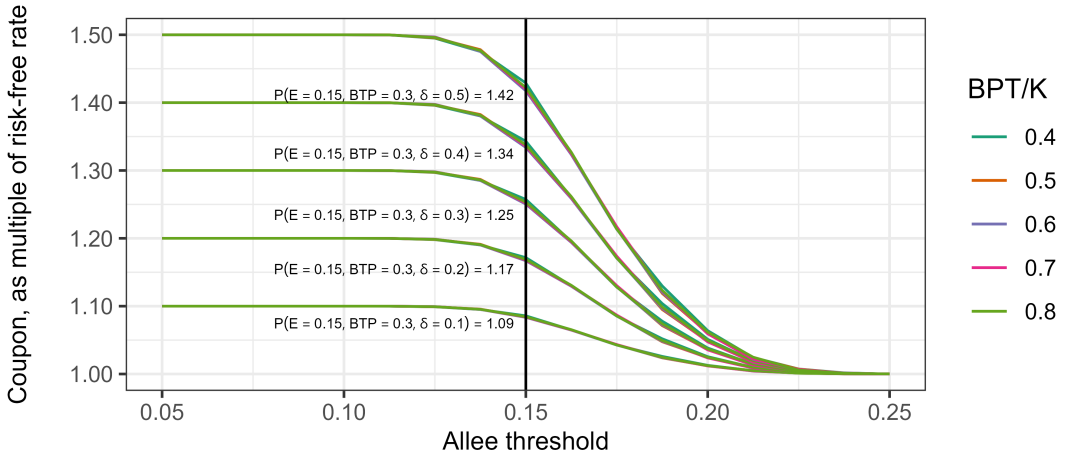

Sources: Hanson and Ryan (1998), Braumann (2019), and the author.
Notes: The figure shows the initial value of the terminal coupon of the BLB for different combinations of the Allee threshold and the biodiversity performance target (BPT), each reported as a fraction of the carrying capacity of the Pacific Halibut ecosystem. The Monte Carlo simulation assumes fixed values of $r^* = r \times T_f = 35.5$, $\sigma^* = r \times \sqrt{T_f} = 1.4$, $\theta^* = \theta \times T_f = 17.75$, $Y_0 = 0.30$, and 10000 replications of equation (4) using the Milstein solution scheme with a 1000 point discretization of the time interval $[0, 1]$.

Figure 5. In-the-money (ITM) probability, BLB step-down coupon: growth rate sensitivity

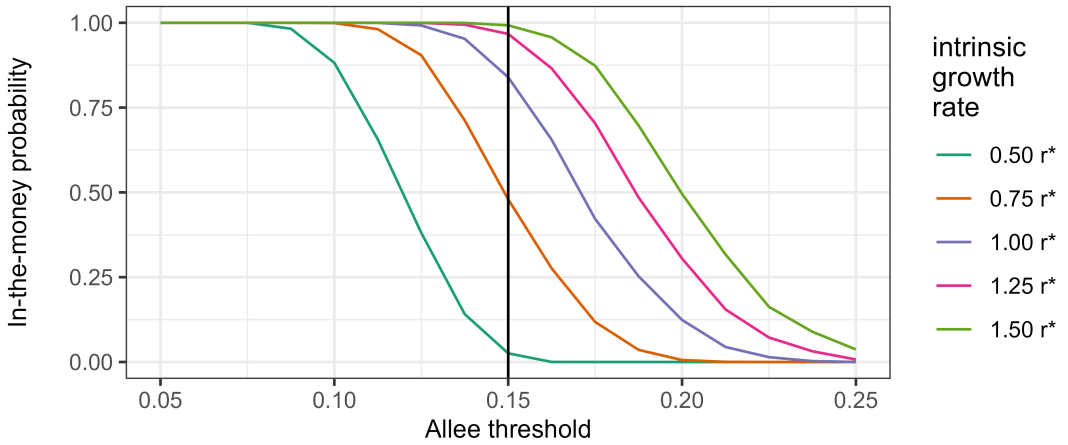

Sources: Hanson and Ryan (1998), Braumann (2019), and the author.
Notes: The figure shows the in-the-money (ITM) probability, or the probability that the step-down coupon will be triggered for different combinations of the Allee threshold and the instantaneous growth rate, the latter reported as a multiple of $r^* = 35.5$. The Monte Carlo simulation assumes fixed values of $K = 1$, $BTP = 0.5$, $\sigma^* = r \times \sqrt{T_f} = 1.4$, $\theta^* = \theta \times T_f = 17.75$, $Y_0 = 0.30$, and 10000 replications of equation (4) using the Milstein solution scheme with a 1000 point discretization of the time interval $[0, 1]$.

Figure 6. In-the-money (ITM) probability, BLB step-down coupon: utilization rate sensitivity

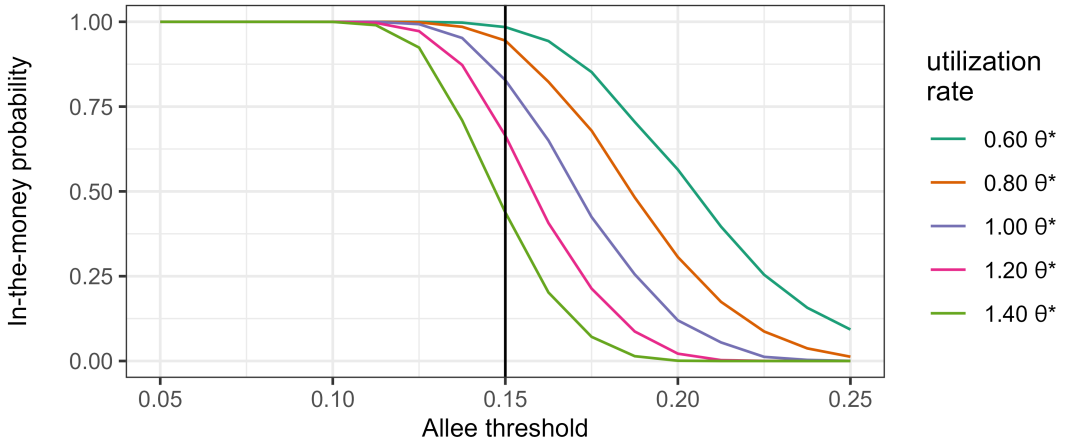

Sources: Hanson and Ryan (1998), Braumann (2019), and the author.
Notes: The figure shows the in-the-money (ITM) probability, or the probability that the step-down coupon will be triggered for different combinations of the Allee threshold and the utilization rate, the latter reported as a multiple of $\theta^* = 17.75$. The Monte Carlo simulation assumes fixed values of $K = 1$, $BTP = 0.5$, $r^* = r \times T_f = 35.5$, $\sigma^* = r \times \sqrt{T_f} = 1.4$, $Y_0 = 0.30$, and 10000 replications of equation (4) using the Milstein solution scheme with a 1000 point discretization of the time interval $[0, 1]$.

Figure 7. In-the-money (ITM) probability, BLB step-down coupon: volatility sensitivity

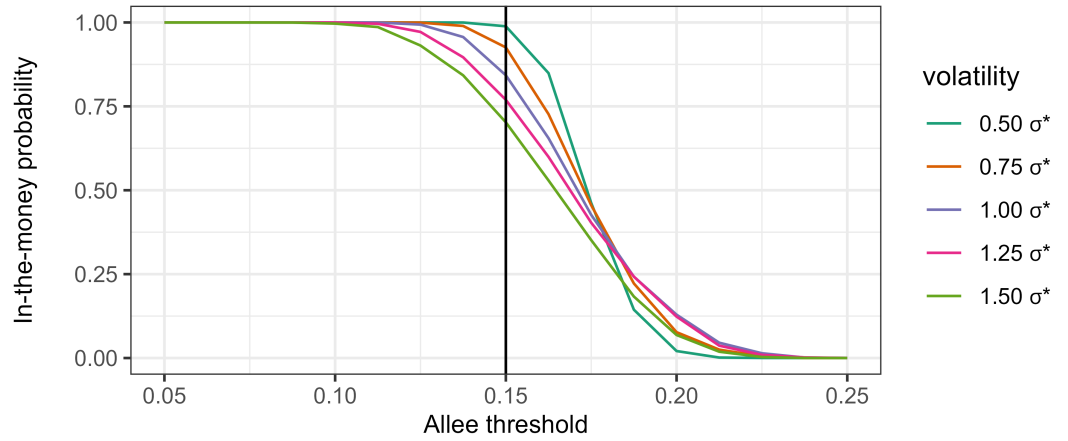

Sources: Hanson and Ryan (1998), Braumann (2019), and the author.
Notes: The figure shows the in-the-money (ITM) probability, or the probability that the step-down coupon will be triggered for different combinations of the Allee threshold and the volatilty parameter, the former reported as a multiple ofthe carrying capacity K, and the latter reported as a multiple of $\sigma^* = 1.4$. The Monte Carlo simulation assumes fixed values of $K = 1$, $BTP = 0.5$, $r^* = r \times T_f = 35.5$, $\theta^* = \theta \times T_f = 17.75$, $Y_0 = 0.30$, and 10000 replications of equation (4) using the Milstein solution scheme with a 1000 point discretization of the time interval $[0, 1]$.

tantial buffer. As the Allee threshold rises, the population dynamics changes as large positive shocks now counterbalance the small initial buffer, driving the population further from extinction and increasing the likelihood of triggering the step-down coupon. Thus, the ITM probability rises with volatility. These outcomes align with option pricing theory: a BLB where the population starts just above the extinction level behaves like a far out-of-the-money option, which benefits from heightened volatility (Black and Scholes 1973; Merton 1973).

The initial value of the biodiversity indicator, the size of the population, buffers the species against the risk of extinction. Higher initial values correspond to higher buffers and make more likely that the step-down coupon will be exercised (Figure 8). For the default Allee threshold, which is 30 percent of the carrying capacity, the ITM probability is 84 percent. Increasing the initial stock value to just 40 percent of the carrying capacity ensures that the step-down coupon will be exercised with certainty over the life of the BLB contract.

Figure 8. In-the-money (ITM) probability, BLB step-down coupon: sensitivity to the initial population size

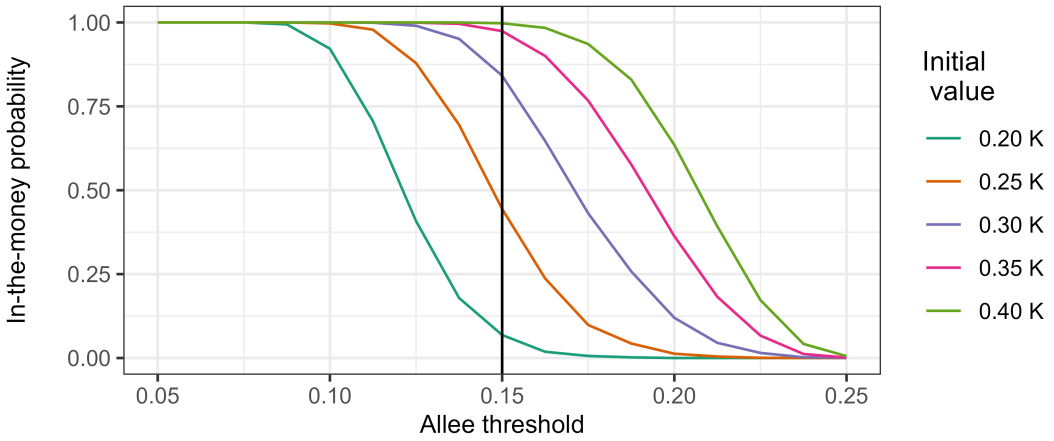

Sources: Hanson and Ryan (1998), Braumann (2019), and the author.
Notes: The figure shows the in-the-money (ITM) probability, or the probability that the step-down coupon will be triggered for different combinations of the Allee threshold and the initial population size, both reported as a multiple of the carrying capaicty K. The Monte Carlo simulation assumes fixed values of $K = 1$, $BTP = 0.5$, $r^* = r \times T_f = 35.5$, $\theta^* = \theta \times T_f = 17.75$, $\sigma^* = 1.4$, $Y_0 = 0.30$, and 10000 replications of equation (4) using the Milstein solution scheme with a 1000 point discretization of the time interval $[0, 1]$.

From the numerical results, we can infer that there are four parameters that significantly influence the success of a BLB, which is to maximize the probability of reaching the BPT. They are the growth rate of the population (or biodiversity indicator) and its volatility, the utilization rate, and the size of the initial population. These parameters, which are linked to the ecosystem health and biodiversity outcomes, can be partially regulated by human intervention. Among them, the utilization rate can be rapidly adjusted, which could have a positive feedback on the growth rate of the population.

The numerical example assumes that the BLB step-down coupon option will mature in 50 years, i.e. $T_f = 50$. Even in the case that a liquid market for long-term BLBs exists, mirroring the market for long-term government bonds in Germany, Japan, and the United States, it might be worth evaluating the possibility of issuing BLBs with shorter maturities. This evaluation requires calculating the first passage time (FPT) of the biodiversity indicator under different assumptions. Given a stochastic process, the first passage time is the random variable the measures the time the process takes to reach a specified level for the first time. In this case, the stochastic process governing the behavior of the biodiversity indicator is characterized by equation 4 and the biodiversity performance target corresponds to the specified level.

Figure 9 displays the distribution of the FPTs for different BPT values, where the distributions are estimated using a gaussian kernel density and the BPT values are expressed as multiples of the carrying capacity, K. The BPT value affects the location and shape of the FPT distributions, in sharp contrast with the ITM probabilities, which are barely affected, as depicted in (3) above. As the BPT increases, the mode (peak) of the density distributions shift to the right since, as expected, it takes longer to reach the BPT for any given biodiversity initial value. Since higher BPTs drive up the duration of the FTP, the likelihood that shocks affect the biodiversity indicator increases, leading to a wider dispersion of the FPT distribution.

Table 1 presents the summary statistics for the FPT distributions across different BPT values. The three location measures (mean, median, and mode) along with the distribution quantiles (minimum, maximum, and the first and third quartiles) indicate that the FPT distribution shifts rightward as the BPT value increases. The second moment, represented by the standard deviation, remains relatively unaffected by changes in the BPT. However, for all BPT values, the FPT distributions are right-skewed and leptokurtic due to heavier tails on the distribution's right side, but the skewness and leptokurtosis diminish as the BPT value increases.

Figure 10 and Table 2 examine how variations in the Allee threshold affect the FPT. The results indicate that higher Allee thresholds correspond to longer FPTs. This is evident in the figure, where lower thresholds lead to faster FPTs, while higher thresholds cause the distributions to become more spread out, indicating a delay in reaching the biodiversity performance target. Recall from equation (4) that the drift rate is inversely proportional to the Allee threshold value due to the factor $(\frac{Y_\tau}{E_K} - 1)$. Low threshold values lead to higher drift values, contributing to faster FPTs.

The summary statistics in Table 2 reinforce these findings. As the Allee threshold increases, the mean, median, and mode of the FPT all rise, signifying that populations take longer to reach the performance target at higher thresholds. The standard deviation also grows with the threshold, showing that the timing becomes more variable. This reflects the longer FPTs, which increase the likelihood that the biodiversity indicator is affected

Figure 9. First passage time, BLB step-down coupon:
biodiversity performance target sensitivity

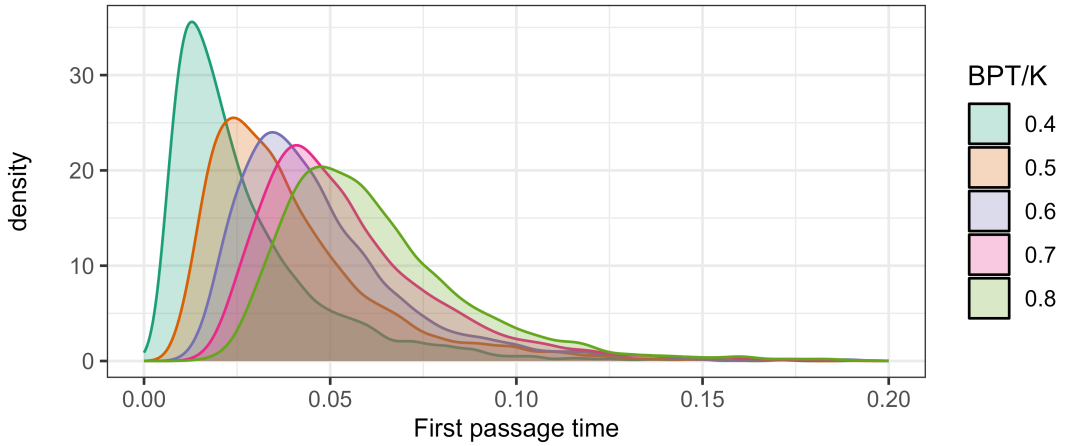

Sources: Hanson and Ryan (1998), Braumann (2019), and the author.
Notes: The figure shows the gaussian kernel density of the first passage time (FPT), which is defined as the first time the biodiversity indicator (population size) reaches or exceeds a biodiversity performance target (BPT) for different values of the BPT. The FPT is reported as a fraction of the time period T_f. The densities are calculated using Monte Carlo Simulation with 10000 replications of equation (4) using the Milstein solution scheme with a 1000 point discretization of the time interval $[0, 1]$, and assuming that $K = 1,\ E = 0.15,\ r^* = r \times T_f = 35.5,\ \sigma^* = r \times \sqrt{T_f} = 1.4,\ \theta^* = \theta \times T_f = 17.75,\ Y_0 = 0.30$.

by shocks. Additionally, higher

Table 1. First passage time, BLB step-down coupon:
biodiversity performance target sensitivity, summary statistics

BPT	mean	median	mode	min	first quartile	third quartile	max	std. dev.	skewness	kurtosis
0.4	0.027	0.021	0.013	0.003	0.013	0.034	0.216	0.022	2.350	11.453
0.5	0.040	0.034	0.024	0.008	0.024	0.049	0.229	0.024	1.840	8.036
0.6	0.048	0.042	0.034	0.011	0.032	0.057	0.213	0.025	2.027	9.359
0.7	0.055	0.049	0.041	0.014	0.038	0.066	0.228	0.026	1.760	7.865
0.8	0.062	0.057	0.048	0.014	0.045	0.074	0.232	0.026	1.682	7.588

Sources: Hanson and Ryan (1998), Braumann (2019), and the author.
Notes: The table presents the summary statistics of the first passage time (FPT), which is defined as the first time the biodiversity indicator (population size) reaches or exceeds a biodiversity performance target (BPT) for different values of the BPT. The FPT is reported as a fraction of the time period T_f, and the statistics are calculated using Monte Carlo Simulation with 10000 replications of equation (4) using the Milstein solution scheme with a 1000 point discretization of the time interval $[0, 1]$, and assuming that $K = 1,\ r^* = r \times T_f = 35.5,\ \sigma^* = r \times \sqrt{T_f} = 1.4,\ \theta^* = \theta \times T_f = 17.75,\ Y_0 = 0.30$.

Figure 10. First passage time, BLB step-down coupon:
Allee threshold sensitivity

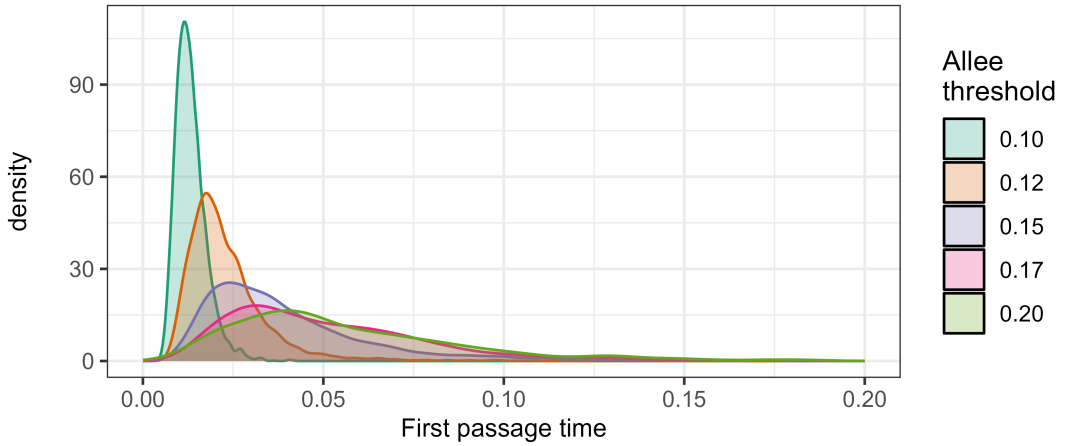

Sources: Hanson and Ryan (1998), Braumann (2019), and the author.
Notes: The figure shows the density of the first passage time (FPT), which is defined as the first time the biodiversity indicator (population size) reaches or exceeds a biodiversity performance target (BPT) for different Allee threshold values expressed as multiples of the carrying capacity. The FPT is reported as a fraction of the time period T_f. The densities are calculated using Monte Carlo Simulation with 10000 replications of equation (4) using the Milstein solution scheme with a 1000 point discretization of the time interval $[0, 1]$, and assuming that $K = 1,\ BPT = 0.5,\ r^* = r \times T_f = 35.5,\ \sigma^* = r \times \sqrt{T_f} = 1.4,\ \theta^* = \theta \times T_f = 17.75,\ Y_0 = 0.30$.

Table 2. First passage time, BLB step-down coupon:
Allee threshold sensitivity, summary statistics

Allee threshold	mean	median	mode	min	first quartile	third quartile	max	std. dev.	skewness	kurtosis
0.100 K	0.013	0.013	0.012	0.004	0.010	0.015	0.042	0.004	1.276	6.195
0.125 K	0.023	0.021	0.018	0.006	0.016	0.027	0.133	0.011	2.582	15.455
0.150 K	0.040	0.034	0.024	0.008	0.024	0.049	0.229	0.024	1.840	8.036
0.175 K	0.053	0.045	0.032	0.011	0.030	0.067	0.287	0.031	1.816	8.700
0.200 K	0.057	0.048	0.040	0.011	0.034	0.073	0.232	0.035	1.612	6.549

Sources: Hanson and Ryan (1998), Braumann (2019), and the author.
Notes: The table presents the summary statistics of the first passage time (FPT), which is defined as the first time the biodiversity indicator (population size) reaches or exceeds a biodiversity performance target (BPT) for different values of the Allee threshold. The FPT is reported as a fraction of the time period T_f, and the statistics are calculated using Monte Carlo Simulation with 10000 replications of equation (4) using the Milstein solution scheme with a 1000 point discretization of the time interval $[0, 1]$, and assuming that $K = 1,\ BPT = 0.5,\ r^* = r \times T_f = 35.5,\ \sigma^* = r \times \sqrt{T_f} = 1.4,\ \theta^* = \theta \times T_f = 17.75,\ Y_0 = 0.30$.

skewness and kurtosis values suggest a greater rightward shift in the distributions for higher thresholds, with longer right tails and flatter peaks. In essence, a higher Allee threshold not only prolongs the time to reach the target but also introduces greater uncertainty.

Turning to intrinsic growth rate sensitivity, Figure 11 shows a contrasting dynamic vis-a-vis the Allee threshold. As the intrinsic growth rate increases, the FPT becomes shorter and more concentrated around earlier times. Higher growth rates, lead to sharper density peaks, indicating that the biodiversity indicator is more likely to meet the BPT quickly. Lower growth rates, on the other hand, result in more spread-out distributions, similar to the effect of a higher Allee threshold, but for different reasons. The faster intrinsic growth rates effectively reduce the time needed for the population to reach the target.

Table 3 summarizes the statistics for the intrinsic growth rate sensitivity. It shows a clear trend of decreasing mean, median, and mode as the growth rate increases, along with reduced standard deviations. This means that populations with higher intrinsic growth rates not only reach the performance target faster but do so with less variability in timing. Unlike the Allee threshold, where increasing values slow down the process and add uncertainty, a higher intrinsic growth rate accelerates the process and makes the timing more predictable. Together, the analyses highlight the opposing effects of the Allee threshold and intrinsic growth rate on the first passage time, with the former delaying and the latter speeding up the achievement of biodiversity goals.

Lower utilization rates lead to a faster rate of change of the biodiversity indicators, as reflected in the drift rates in any of the SDEs (1) to (6). Hence, the densities are similar to those of other factors that have a similar effect on the drift rate, such as the Allee threshold (lower thresholds, shorter FPTs) and the intrinsic growth rate (higher rates, shorter FPTs), exhibiting higher and narrower peaks compared with the more spread-out densities corresponding to high utilization rates. This pattern is further supported by the summary statistics reported in Table 4, which show increasing means, medians, and standard deviations as the utilization rate increases. The shape characteristics of these densities provide additional insights into the nature of the FPT across different utilization rates.

All densities exhibit positive skewness, indicating a tendency for longer tails on the right side, which represents occasional instances of significantly delayed first passage times. However, this skewness decreases with higher utilization rates, as does the kurtosis, suggesting that higher rates not only extend the average time to reach the performance target but also make the occurrence of long FPTs more common. Since the utilization rate is under direct human control, this could have important implications for biodiversity conservation strategies, as it suggests that higher utilization rates not only slow down recovery or growth on average but also make the process less predictable, potentially complicating ecological management and policy decisions.

Figure 11. First passage time, BLB step-down coupon: intrinsic growth rate sensitivity

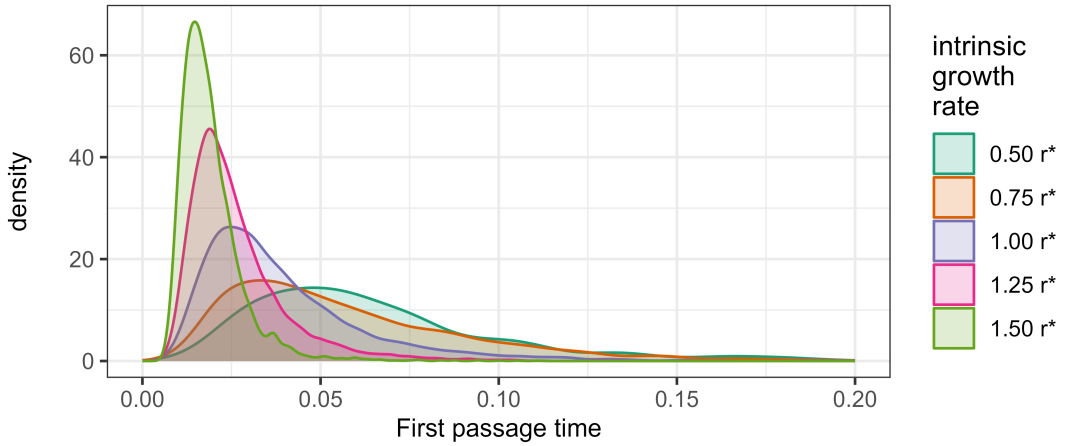

Sources: Hanson and Ryan (1998), Braumann (2019), and the author.
Notes: The figure shows the density of the first passage time (FPT), which is defined as the first time the biodiversity indicator (population size) reaches or exceeds a biodiversity performance target (BPT) for different intrinsic growth rate values. The FPT is reported as a fraction of the time period T_f. The densities are calculated using Monte Carlo Simulation with 10000 replications of equation (4) using the Milstein solution scheme with a 1000 point discretization of the time interval $[0, 1]$, and assuming that $K = 1,\ BPT = 0.5,\ r^* = r \times T_f = 35.5,\ \sigma^* = r \times \sqrt{T_f} = 1.4,\ \theta^* = \theta \times T_f = 17.75,\ Y_0 = 0.30$.

Table 3. First passage time, BLB step-down coupon: intrinsic growth rate sensitivity, summary statistics

intrinsic growth rate	mean	median	mode	min	first quartile	third quartile	max	std. dev.	skewness	kurtosis
0.50 r^*	0.065	0.057	0.048	0.013	0.040	0.079	0.233	0.036	1.441	5.492
0.75 r^*	0.057	0.049	0.033	0.009	0.032	0.074	0.250	0.035	1.450	5.769
1.00 r^*	0.040	0.033	0.025	0.008	0.023	0.048	0.274	0.025	2.423	13.441
1.25 r^*	0.027	0.023	0.019	0.006	0.017	0.031	0.178	0.014	2.228	11.713
1.50 r^*	0.019	0.017	0.015	0.006	0.013	0.022	0.111	0.009	2.740	17.464

Sources: Hanson and Ryan (1998), Braumann (2019), and the author.
Notes: The table presents the summary statistics of the first passage time (FPT), which is defined as the first time the biodiversity indicator (population size) reaches or exceeds a biodiversity performance target (BPT) for different values of the intrinsic growth rate. The FPT is reported as a fraction of the time period T_f, and the statistics are calculated using Monte Carlo Simulation with 10000 replications of equation (4) using the Milstein solution scheme with a 1000 point discretization of the time interval $[0, 1]$, and assuming that $K = 1,\ BPT = 0.5,\ E = 0.15,\ r^* = r \times T_f = 35.5,\ \sigma^* = r \times \sqrt{T_f} = 1.4,\ \theta^* = \theta \times T_f = 17.75,\ Y_0 = 0.30$.

Figure 12. First passage time, BLB step-down coupon: utilization rate sensitivity

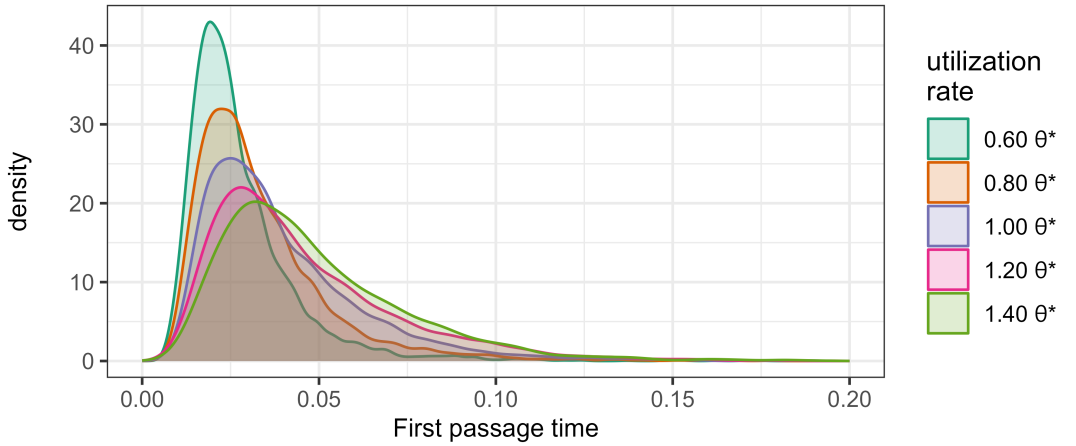

Sources: Hanson and Ryan (1998), Braumann (2019), and the author.
Notes: The figure shows the density of the first passage time (FPT), which is defined as the first time the biodiversity indicator (population size) reaches or exceeds a biodiversity performance target (BPT) for different utilization rate values. The FPT is reported as a fraction of the time period T_f. The densities are calculated using Monte Carlo Simulation with 10000 replications of equation (4) using the Milstein solution scheme with a 1000 point discretization of the time interval $[0, 1]$, and assuming that $K = 1,\ BPT = 0.5,\ r^* = r \times T_f = 35.5,\ \sigma^* = r \times \sqrt{T_f} = 1.4,\ \theta^* = \theta \times T_f = 17.75,\ Y_0 = 0.30$.

Table 4. First passage time, BLB step-down coupon: utilization rate sensitivity, summary statistics

utilization rate	mean	median	mode	min	first quartile	third quartile	max	std. dev.	skewness	kurtosis
0.3 θ^*	0.028	0.024	0.019	0.006	0.018	0.033	0.175	0.016	2.663	15.313
0.4 θ^*	0.033	0.028	0.022	0.007	0.021	0.040	0.221	0.020	2.437	13.516
0.5 θ^*	0.040	0.034	0.025	0.007	0.024	0.049	0.237	0.023	1.942	9.152
0.6 θ^*	0.045	0.038	0.028	0.008	0.027	0.058	0.239	0.027	1.679	7.501
0.7 θ^*	0.049	0.042	0.032	0.008	0.030	0.061	0.264	0.028	1.872	9.535

Sources: Hanson and Ryan (1998), Braumann (2019), and the author.
Notes: The table presents the summary statistics of the first passage time (FPT), which is defined as the first time the biodiversity indicator (population size) reaches or exceeds a biodiversity performance target (BPT) for different values of the utilization rate as a multiple of θ^*. The FPT is reported as a fraction of the time period T_f, and the statistics are calculated using Monte Carlo Simulation with 10000 replications of equation (4) using the Milstein solution scheme with a 1000 point discretization of the time interval $[0, 1]$, and assuming that $K = 1,\ BPT = 0.5,\ E = 0.15,\ r^* = r \times T_f = 35.5,\ \sigma^* = r \times \sqrt{T_f} = 1.4,\ \theta^* = \theta \times T_f = 17.75,\ Y_0 = 0.30$.

Building upon the previous analysis of utilization rate sensitivity, the analysis turns now to the effects of the intrinsic volatility and the initial population size on the FPT. Figure 13 and Table 5 illustrates the impact of the intrinsic volatility on the FPT. Interestingly, unlike with utilization rates, increasing volatility does not uniformly increase the mean FPT. The highest mean FPT occurs at moderate volatility levels, while both lower and higher volatilities result in slightly lower mean FPTs. This suggests a non-linear relationship between the intrinsic volatility and the FPT. However, higher volatility levels do lead to increased standard deviation, indicating greater uncertainty in outcomes. The density plots show that lower volatility results in a more peaked distribution, while higher volatilities lead to flatter, more spread-out distributions. This is further reflected in the decreasing kurtosis values as volatility increases, dropping from 21.441 at 0.50 σ^* to 8.125 at 1.50 σ^*.

Figure 14 and Table 6 reveal the sensitivity of FPT to the initial population size, Y_0. There is a clear inverse relationship between the initial population size and FPT as the gap with the BPT is wider the lower the population size is. This pattern is visually evident in the figure, where the density distributions for higher initial values are concentrated closer to zero on the x-axis. The standard deviation also decreases with higher initial values, indicating more consistent outcomes. However, the skewness increases with higher initial values, suggesting that while FPTs are generally shorter, there's a higher probability of occasional extreme values relative to the mean.

These findings paint a complex picture of how various factors influence the time it takes for a biodiversity indicator to reach or exceed a performance target. The non-linear effect of volatility suggests that moderate levels of environmental variability might actually delay recovery or growth more than extreme volatility. Meanwhile, the strong influence of initial population size highlights the importance of preserving biodiversity, as populations starting closer to their target levels are much more likely to reach performance goals quickly. These insights could be valuable for conservation strategies, suggesting that efforts to stabilize environments at moderate levels and maintain population sizes above critical thresholds could be more effective than focusing solely on minimizing volatility or maximizing population sizes.

From a contract design perspective, the results suggest that despite the long horizons biodiversity entails, such as 50 years in this numerical example, it is feasible to design contracts with maturities well below the biodiversity horizon regardless of the selected BPT. For none of the BPT values considered, the FPT exceeds one quarter of the biodiversity horizon, which amounts to $12\frac{1}{2}$ years. A short duration contract does not imply that the risk of the contract ending out-of-the money, i.e. the biodiversity indicator never reaches the BPT, is negligible. The results shown in Figure 9 and Table 1 correspond to those replications in the Monte Carlo simulation that reached the BPT. The probability that the ecosystem fails, keeping the default parameter values fixed, is 16 percent.

Figure 13. First passage time, BLB step-down coupon: volatility sensitivity

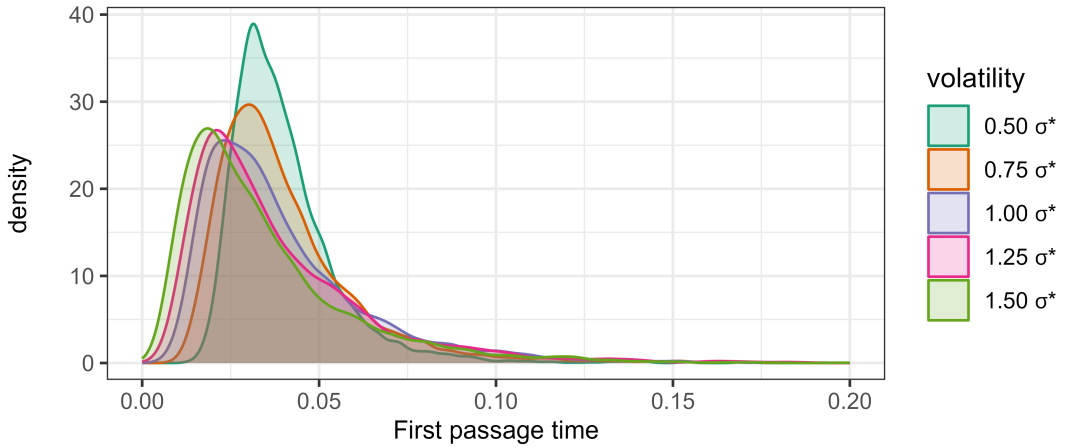

Sources: Hanson and Ryan (1998), Braumann (2019), and the author.
Notes: The figure shows the density of the first passage time (FPT), which is defined as the first time the biodiversity indicator (population size) reaches or exceeds a biodiversity performance target (BPT) for different volatility values. The FPT is reported as a fraction of the time period T_f. The densities are calculated using Monte Carlo Simulation with 10000 replications of equation (4) using the Milstein solution scheme with a 1000 point discretization of the time interval $[0, 1]$, and assuming that $K = 1$, $BPT = 0.5$, $r^* = r \times T_f = 35.5$, $\sigma^* = r \times \sqrt{T_f} = 1.4$, $\theta^* = \theta \times T_f = 17.75$, $Y_0 = 0.30$.

Table 5. First passage time, BLB step-down coupon: intrinsic volatility sensitivity, summary statistics

intrinsic volatility	mean	median	mode	min	first quartile	third quartile	max	std. dev.	skewness	kurtosis
0.50 σ^*	0.040	0.037	0.032	0.013	0.030	0.046	0.247	0.016	2.961	21.441
0.75 σ^*	0.041	0.035	0.030	0.010	0.027	0.048	0.230	0.021	2.276	11.676
1.00 σ^*	0.040	0.033	0.023	0.008	0.023	0.049	0.231	0.025	2.022	9.207
1.25 σ^*	0.038	0.030	0.021	0.005	0.021	0.048	0.273	0.026	2.105	9.916
1.50 σ^*	0.035	0.028	0.018	0.005	0.018	0.043	0.210	0.025	1.919	8.125

Sources: Hanson and Ryan (1998), Braumann (2019), and the author.
Notes: The table presents the summary statistics of the first passage time (FPT), which is defined as the first time the biodiversity indicator (population size) reaches or exceeds a biodiversity performance target (BPT) for different values of the intrinsic volatility as a multiple of θ^*. The FPT is reported as a fraction of the time period T_f, and the statistics are calculated using Monte Carlo Simulation with 10000 replications of equation (4) using the Milstein solution scheme with a 1000 point discretization of the time interval $[0, 1]$, and assuming that $K = 1$, $BPT = 0.5$, $E = 0.15$, $r^* = r \times T_f = 35.5$, $\sigma^* = r \times \sqrt{T_f} = 1.4$, $\theta^* = \theta \times T_f = 17.75$, $Y_0 = 0.30$.

Figure 14. First passage time, BLB step-down coupon:
sensitivity to the initial population size

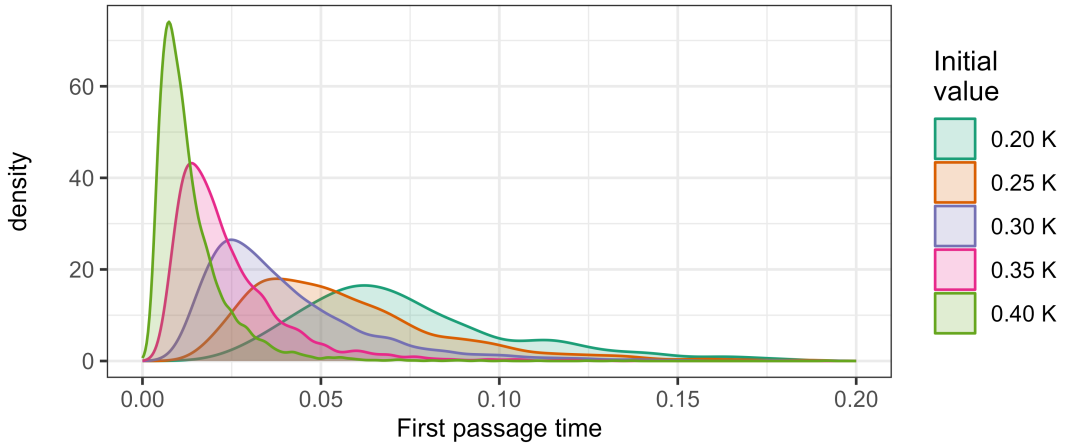

Sources: Hanson and Ryan (1998), Braumann (2019), and the author.
Notes: The figure shows the density of the first passage time (FPT), which is defined as the first time the biodiversity indicator (population size) reaches or exceeds a biodiversity performance target (BPT) for different volatility values. The FPT is reported as a fraction of the time period T_f. The densities are calculated using Monte Carlo Simulation with 10000 replications of equation (4) using the Milstein solution scheme with a 1000 point discretization of the time interval $[0, 1]$, and assuming that $K = 1$, $BPT = 0.5$, $r^* = r \times T_f = 35.5$, $\sigma^* = r \times \sqrt{T_f} = 1.4$, $\theta^* = \theta \times T_f = 17.75$, $Y_0 = 0.30$.

Table 6. First passage time, BLB step-down coupon:
initial value Y_0 sensitivity, summary statistics

initial Y_0	mean	median	mode	min	first quartile	third quartile	max	std. dev.	skewness	kurtosis
0.20 K	0.076	0.069	0.062	0.024	0.054	0.090	0.242	0.034	1.626	7.106
0.25 K	0.058	0.051	0.037	0.013	0.037	0.070	0.269	0.029	1.586	6.992
0.30 K	0.040	0.034	0.025	0.007	0.024	0.050	0.217	0.024	2.073	9.835
0.35 K	0.024	0.020	0.014	0.004	0.014	0.030	0.223	0.016	2.619	15.823
0.40 K	0.014	0.011	0.007	0.002	0.007	0.017	0.192	0.011	3.867	35.267

Sources: Hanson and Ryan (1998), Braumann (2019), and the author.
Notes: The table presents the summary statistics of the first passage time (FPT), which is defined as the first time the biodiversity indicator (population size) reaches or exceeds a biodiversity performance target (BPT) for different values of the initial value of the biodiversity indicator, Y_0 as a multiple of K. The FPT is reported as a fraction of the time period T_f, and the statistics are calculated using Monte Carlo Simulation with 10000 replications of equation (4) using the Milstein solution scheme with a 1000 point discretization of the time interval $[0, 1]$, and assuming that $K = 1$, $BPT = 0.5$, $E = 0.15$, $r^* = r \times T_f = 35.5$, $\sigma^* = r \times \sqrt{T_f} = 1.4$, $\theta^* = \theta \times T_f = 17.75$.

5 Conclusions

Ecosystems are integral to the global economy, supporting about half of global GDP (US$ 44 trillion) in 2020. However, many governments, especially in developing countries rich in biodiversity, lack the resources to effectively manage and conserve these ecosystems due to competing priorities and limited budgets. This creates a pressing need for private sector engagement. Private capital, particularly from institutional investors seeking sustainable returns, is essential for bridging the biodiversity funding gap. Mobilizing these resources can help ensure the long-term preservation of biodiversity, which is crucial not only for local environments but also for global economic stability.

Biodiversity-linked bonds (BLBs) offer an innovative approach to engaging the private sector in conservation efforts. Similar to sustainability-linked bonds (SLBs), which have successfully supported net-zero carbon initiatives, BLBs could align investor returns with specific biodiversity outcomes, such as species protection and habitat restoration. These bonds provide flexibility for issuers while offering investors a meaningful way to contribute to conservation. With the growing demand for sustainable investment opportunities, BLBs can tap into private capital markets to fund biodiversity initiatives that are often beyond the financial capacity of the public sector. To fully realize the potential of BLBs, a robust valuation framework must be established.

The contribution of this paper to the growing literature on biodiversity is the introduction of a novel valuation framework for BLBs. The framework builds on and adapts existing option pricing methodologies for sustainability-linked bonds (SLBs) to incorporate key characteristics of biological and ecological models of biodiversity growth. The framework accounts for an ecosystem carrying capacity and the Allee effect, or risk of extinction when biodiversity falls below critical thresholds, making it particularly suited for conservation-focused financial instruments. Additionally, the model integrates human activities, recognizing their direct and indirect impact on biodiversity dynamics, and offers practical tools for evaluating BLB risk-return profiles. This approach provides both a theoretical foundation and a practical framework for the design and assessment of biodiversity-related financial products, addressing the urgent need for innovative mechanisms to finance global conservation efforts. Furthermore, the proposed framework could complement existing policy guidelines and principles designed to promote biodiversity, such as those proposed by Parker et al. (2012), the ADB and IFC (2023), and Nature Finance and FGV (2024), among others, and could help to align financial incentives with conservation goals and supporting broader biodiversity initiatives.

Building on its valuation principles, the proposed valuation framework also serves as a tool to identify the key factors that drive the success of a BLB contract. The primary goal of a BLB issuer is to achieve a predefined biodiversity performance target (BPT). When these targets align with positive biodiversity outcomes, both the issuer and the investor share an interest in ensuring the embedded options in the BLB are exercised, or in-the-

money. Several factors drive the likelihood of success for the BLB, with the most critical being the value of the BPT, the growth rate and volatility of the biodiversity indicator, the utilization rate of the biodiversity contract, and the initial value of the biodiversity indicator. By simulating the BLB contract using realistic parameter values, the framework allows for a clear assessment of the relative importance of each factor in determining the contract's success and its ability to meet the needs of issuers and investors alike. As an example, the approach was applied to a binary BLB step-down coupon option. The numerical analysis showed how the coupon of the BLB depended on the values of the BPT, and the role the remaining factors in determining the likelihood of the step-down option being exercised. In particular, a higher utilization rate by humans could impair an ecosystem abiity to recover successfully. In addition, the added uncertainty associated with higher utilization rates might add further complications to ecological management and policy decisions.

Ultimately, the integration of biodiversity into financial markets through instruments like BLBs represents a crucial step toward bridging the gap between conservation and capital, and could encourage further work on the valuation of nature, both in terms of modeling work (Barbier 2011, Fenichel and Abbott 2014, Fenichel, Abbott, and Yun 2018) and practical applications (AIIB 2023). As pressures on ecosystems grow, innovative financial mechanisms that align private sector interests with global biodiversity goals are not just a promising idea—they are an urgent necessity. The valuation framework proposed here lays the groundwork for unlocking the full potential of BLBs, offering a structured path for both issuers and investors to contribute meaningfully to biodiversity preservation. By aligning financial returns with ecological sustainability, BLBs can become a cornerstone in the fight to safeguard our planet's most vital natural assets.

References

Allee, Warder Clyde. 1931. *Animal Aggregations: a Study in General Sociology.* Chicago, IL: University of Chicago Press.

Amarti, Zenia, Neden S. Nurkholipah, Nursanti Anggriani, and Asep K. Supriatna. 2018. "A Gompertz Population Model with Allee Effect and Fuzzy Initial Values." *Symposium on Biomathematics (SYMOMATH) 2017, AIP Conference Proceedings* 1937. https://doi.org/10.1063/1.5026074.

Andrikopoulos, Andreas, and Andrianos E. Tsekrekos. 2024. "The Pay-for-Success Contract: a Valuation Note." *Journal of Futures Markets* 44 (9): 1465–1473. https://doi.org/10.1002/fut.22534.

ASEAN Centre for Biodiversity. 2023. ASEAN Biodiversity Outlook 3. Philippines. https://www.aseanbiodiversity.org/asean-biodiversity-outlook/.

Asian Development Bank and International Finance Corporation. 2023. Bonds to Finance the Sustainable Blue Economy: a Practitioner's Guide. Technical report. Manila, Philippines. https://www.icmagroup.org/assets/documents/Sustainable-finance/Bonds-to-Finance-the-Sustainable-Blue-Economy-a-Practitioners-Guide-September-2023.pdf.

Bank, Asian Infrastructure Investment. 2023. Asian Infrastructure Finance 2023: Nature as Infrastructure. Technical report. Beijing, China. https://www.aiib.org/en/news-events/asian-infrastructure-finance/_common/pdf/AIIB-Asian-Infrastructure-Finance-2023-Report.pdf.

Barbier, Edward B. 2011. *Capitalizing on Nature: Ecosystems as Natural Assets.* Cambridge, UK: Cambridge University Press.

Berg, Florian, Julian F. Koelbel, and Roberto Rigobon. 2022. "Aggregate Confusion: the Divergence of ESG Ratings." *Review of Finance* 26 (6): 1315–1344. https://doi.org/10.1093/rof/rfac033.

Black, Fischer, and Myron S. Scholes. 1973. "The Pricing of Options and Corporate Liabilities." *Journal of Political Economy* 81 (3): 637–654. https://www.journals.uchicago.edu/doi/10.1086/260062.

Block, Sebastian, John W. Emerson, Daniel C. Esty, Alex de Sherbinin, and Zachary A. Wendling. 2024. Environmental Performance Index. New Haven, CT: Yale Center for Environmental Law & Policy. https://epi.yale.edu/downloads/2024-epi-report.pdf.

Braumann, Carlos A. 2019. *Introduction to Stochastic Differential Equations with Applications to Modelling in Biology and Finance.* Hoboken, NJ: John Wiley & Sons.

Brites, Nuno M. 2017. "Stochastic Differential Equation Harvesting Models: Sustainable Policies and Profit Maximization." PhD thesis, Universidade de Evora. https://www.proquest.com/openview/d4d1411098c176aa4dbe7722359ae3ef/1?pq-origsite=gscholar&cbl=2026366&diss=y.

Capocelli, Renato M., and Luigi M. Ricciardi. 1974. "A Diffusion Model for Population Growth in Random Environment." *Theoretical Population Biology* 5:28–41. https://doi.org/10.1016/0040-5809(74)90050-1.

Carlos, Clara, and Carlos A. Braumann. 2017. "General Population Growth Models with Allee Effects in a Random Environment." *Ecological Complexity* 30:26–33. https://doi.org/10.1016/j.ecocom.2016.09.003.

Chen, An, Maria Hinken, and Gunter Loffler. 2024. Valuation and Design of Sustainability-Linked Bonds. Technical report. Ulm, Germany: Ulm University. https://papers.ssrn.com/sol3/Delivery.cfm/SSRN_ID4787776_code5863319.pdf?abstractid=4657071&mirid=1.

Cheng, Gong, Torsten Ehlers, and Frank Packer. 2022. "Sovereigns and Sustainable Bonds: Challenges and New Options." *BIS Quarterly Review,* 47–55. https://www.bis.org/publ/qtrpdf/r_qt2209d.pdf.

Chouhan, Neeraj, Caroline Harrison, and Deepak Sharma. 2024. Sustainable Debt: Global State of the Market. Technical report. London, UK: Climate Bonds Initiatitve. https://www.climatebonds.net/files/reports/cbi_sotm23_02h.pdf#page=20.07.

Conservation International. 2024. "Biodiversity Hotspots." https://www.conservation.org/priorities/biodiversity-hotspots.

Credit Suisse, World Wildlife Fund, and McKinsey Center for Business and Environment. 2014. Conservation Finance: Moving Beyond Donor Funding Toward an Investor-Driven Approach. Technical report. https://www.cbd.int/financial/privatesector/g-private-wwf.pdf.

Credit Suisse and McKinsey Center for Business and Environment. 2016. Conservation Finance, from Niche to Mainstream - the Building of an Institutional Asset Class. Technical report. https://www.sprep.org/attachments/VirLib/Global/conservation-finance.pdf.

Dasgupta, Partha. 2021. The Economics of Biodiversity: the Dasgupta Review. London, U.K.: HM Treasury. https://assets.publishing.service.gov.uk/media/602e92b2e90e07660f807b47/The_Economics_of_Biodiversity_The_Dasgupta_Review_Full_Report.pdf.

Davis, M.H.A. 1999. "Option Valuation and Hedging with Basis Risk." In *System Theory: Modeling, Analysis and Control,* edited by T.E. Djaferis and I.C. Schick. Amsterdam: Kluwer.

de Mariz, Frederic, Pieter Bosmans, Daniel Leal, and Saumya Bisaria. 2024. "Reforming Sustainability-Linked Bonds by Strengthening Investor Trust." *Journal of Risk and Financial Management* 17 (290). https://doi.org/10.3390/jrfm17070290.

Deutz, Andrew, Geoffrey M. Heal, Rose Inu, Eric Swanson, Eric Townshend, Zhu Li, Alejandro Delmar, Alqayam Meghji, suresh A. Sethi, and John Tobin-de la Puente. 2020. Financing Nature: Closing the Global Biodiversity Financing Gap. Paulson Institute, the Nature Conservancy, and the Conrell Atkinson Center for Substainability. https://www.paulsoninstitute.org/wp-content/uploads/2020/10/FINANCING-NATURE_Full-Report_Final-with-endorsements_101420.pdf.

Du, Kai, Jarrad Harford, and David (Dongcheon) Shin. 2024. Who Benefits from Sustainability-Linked Loans? Finance Working Paper 917/2023. European Corporate Governance Institute. https://papers.ssrn.com/sol3/papers.cfm?abstract_id=4260717.

Erlandsson, Ulf, Josephine Richardson, with Stephanie Mielnik, Kamesh Korangi, Cedric Rimaud, Johan Jarnmo, David Lewis, and Hazel Llango. 2024. *Sustainability-Linked Bond Handbook: A Practitioner's Guide.* London, UK: Anthropocene Fixed Income Institute.

Feldhutter, Peter, Kristoffer Halskov, and Arthur Krebbers. 2024. "Pricing of Sustainability-Linked Bonds." *Journal of Financial Economics* 162 (103944). https://doi.org/10.1016/j.jfineco.2024.103944.

Fenichel, Eli P., and Joshua K. Abbott. 2014. "Natural Capital: from Metaphor to Measurement." *Journal of the Association of Environmental and Resource Economists* 1, nos. 1/2 (May-June): 1–27. https://doi.org/10.1086/676034.

Fenichel, Eli P., Joshua K. Abbott, and Seong Do Yun. 2018. "The Nature of Natural Capital and Ecosystem Income." In *Handbook of Environmental Economics,* edited by Partha Dasgupta, Subhrendu K. Pattanayak, and V. Kerry Smith, 4:85–142. Amsterdam: Elsevier B.V. https://www.sciencedirect.com/science/article/abs/pii/S1574009918300020.

Flammer, Caroline, Thomas Giroux, and Geoffrey M. Heal. 2025. "Biodiversity Finance." *Journal of Financial Economics,* no. 103987, https://doi.org/10.1016/j.jfineco.2024.103987.

G20 Strategies, The Global Bioeconomy: Preliminary Stocktake of, and Practices. 2024. Technical report. https://www.naturefinance.net/wp-content/uploads/2024/05/ENG-TheGlobalBioeconomy_FINAL.pdf.

Giglio, Stefano, Theresa Kuchler, Johannes Stroebel, and Oliver Wang. 2024. The Economics of Biodiversity Loss. NBER Working Paper 32678. Cambridge, MA: National Bureau of Economic Research. https://www.nber.org/papers/w32678.

Hanson, Floyd B., and Dennis Ryan. 1998. "Optimal Harvesting with both Population and Price Dynamics." *Mathematical Biosciences* 148 (2): 129–146. https://homepages.math.uic.edu/~hanson/pub/Price/price97web.pdf.

Haq, Ul Imtiaz, and Djeneba Doumbia. 2022. Structural Loopholes in Sustainability-Linked Bonds. Policy Research Working Paper 10200. Washington, DC: World Bank Group, International Finance Corporation. https://documents1.worldbank.org/curated/en/099237410062223046/pdf/IDU0e099a50307f86045a80b33201d0b7057cedf.pdf.

Herweijer, Celine, Will Evison, Samra Mariam, Akanksha Khatri, Marco Albani, Alexia Semov, and Euan Long. 2020. Nature Risk Rising: Why the Crisis Engulfing Nature Matters for Business and the Economy, New Nature Economy Series. Geneva, Switzerland: World Economic Forum. http://www3.weforum.org/docs/WEF_New_Nature_Economy_Report_2020.pdf.

Hoekstra, Jonathan M., Jennifer Molnar, Carmen Revenga, Mark D. Spalding, Timoty M. Boucher, James C. Robertson, Thomas J. Heibel, and Katherine Ellison. 2010. *The Atlas of Global Conservation.* Berkeley and Los Angeles, CA: University of California Press.

International Capital Markets Association. 2024. Sustainability-Linked Bond Principles: Voluntary Process Guidelines. Paris, France. https://www.icmagroup.org/assets/documents/Sustainable-finance/2024-updates/Sustainability-Linked-Bond-Principles-June-2024.pdf.

Jiang, Daqing, Ningzhong Shi, and Yanan Zhao. 2005. "Existence, Uniqueness and global Stability of Positive solutions to the Food-Limited Population with Random Perturbation." *Mathematical and Computer Modelling* 42 (5-6): 651–658. https://doi.org/10.1016/j.mcm.2004.03.011.

Karolyi, G. Andrew, and John Tobin-de la Puente. 2023. "Biodiversity Finance: a Call for Research into Financing Nature." *Financial Management* 52 (2): 231–251. https://doi.org/10.1111/fima.12417.

Kloeden, Peter E., and Eckhard Platen. 1999. *Numerical Solution of Stochastic Differential Equations.* Second edition. Berlin and New Yok: Springer.

Kolbel, Julian F., and Adrien-Paul Lambillon. 2023. Who Pays for Sustainabilty? An Analysis of Sustainabilty-Linked Bonds. Working Paper. University of St. Gallen, MIT Sloan, Swiss Finance Institute, University of Zurich. https://papers.ssrn.com/sol3/papers.cfm?abstract_id=4007629.

Krstic, Marija, and Miljana Jovanovic. 2010. "On Stochastic Population Model with the Allee Effect." *Mathematical and Computer Modelling* 52 (1-2): 370–379. https://doi.org/10.1016/j.mcm.2010.02.051.

Lam, Pauline, and Jeffrey Wurgler. 2024. Green Bonds: New Label, Same Projects. NBER Working Paper 32960. Cambridge, MA: National Bureau of Economic Research.

Levins, Richard. 1969. "The Effect of Random Variations of Different Types on Population Growth." *Proceedings of the National Academy of Sciences* 62 (4): 1061–1965. https://doi.org/10.1073/pnas.62.4.1061.

Maron, Martine et al. 2023. "'Nature positive' must incorporate, not undermine, the mitigation hierarchy." *Nature Ecology & Evolution* 8:14–17. nature.com/articles/s41559-023-02199-2.

Medina, Claire, and Ivan R. Scales. 2024. "Finance and Biodiversity Conservation: Insights from Rhinoceros Conservation and the First Wildlife Conservation Bond." *Oryx* 1:90–99. https://doi.org/10.1017/S0030605322001648.

Merton, Robert C. 1973. "The Theory of Rational Option Pricing." *Bell Journal of Economics and Management Science* 4 (1): 141–183. https://doi.org/10.2307/3003143.

Mielnik, Stephanie, and Ulf G. Erlandsson. 2022. An Option Pricing Approach to Sustainability-Linked Bonds. London, UK: Anthropocene Fixed Income Institute. https://anthropocenefii.org/downloads/AFII_An-option-pricing-approach-for-sustainability-linked-bonds.pdf.

Millenium Ecosystem Assessment. 2005. *Ecosystems and Human Well-Being Synthesis.* Washington, DC.: Island Press. https://www.millenniumassessment.org/documents/document.356.aspx.pdf.

Murphy, Daniel. 2022. "What are Sustainability Linked Bonds and How Can They Support the Net-Zero Transition." https://www.weforum.org/agenda/2022/11/cop27-sustainability-linked-bonds-net-zero-transition/.

Oksendal, Bernt. 2013. *Stochastic Differential Equations: an Introduction with Applications.* Sixth edition. Berlin and New York: Springer.

Padin-Dujon, Alejandra, and Ben Filewood. 2023. "What are Sustainability-Linked Bonds and How Can They Help Developoing Countries." https://www.lse.ac.uk/granthaminstitute/explainers/what-are-sustainability-linked-bonds-and-how-can-they-help-developing-countries/.

Parker, Charlie, Matthew Cranford, Nick Oakes, and Matt Leggett, eds. 2012. *The Little Biodiversity Finance Book.* Oxford: Global Canopy Programme. https://www.cbd.int/financial/hlp/doc/literature/LittleBiodiversityFinanceBook_3rd%20edition.pdf.

Saha, Bapi, Amiya R. Bhowmick, Joydev Chattopadhyay, and Sabyasachi Bhattacharya. 2013. "On the Evidence of an Allee Effect in Herring Populations and Consequences for Population Survival: A Model-Based Study." *Ecological Modelling* 250:72–80. https://doi.org/10.1016/j.ecolmodel.2012.10.021.

Sau, Anurag, Bapi Saha, and Sabyasachi Bhattacharya. 2020. "An Extended Stochastic Allee Model with Harvesting and the Risk of Extinction of the Herring Population." *Journal of Theoretical Biology* 503. https://doi.org/10.1016/j.jtbi.2020.110375.

Skiadas, Christos H. 2010. "Exact Solutions of Stochastic Differential Equations: Gompertz, Generalized Logistic and Revised Exponential." *Methodology and Computing in Applied Probability* 12 (2): 261–270. https://link.springer.com/article/10.1007/s11009-009-9145-3.

Taylor, M.Scott, and Rolf Weder. 2023. On the Economics of Extinction and Mass Extinctions. NBER Working Paper 31953. Cambridge, MA: National Bureau of Economic Research. https://doi.org/10.3386/w31952.

———. 2024. "On the Economics of Extinction and Possible Mass Extinctions." *Journal of Economic Perspectives* 38 (3): 237–259. https://doi.org/10.1257/jep.38.3.237.

United Nations Framework Convention on Climate Change. 2022. Fift Biennial Assessment and Overview of Climate Finance Flows - Summary and Recommendations by the Standing Committee on Finance. New York, NY: United Nations. https://unfccc.int/sites/default/files/resource/J0156_UNFCCC%20BA5%202022%20Summary_Web_AW.pdf.

World Bank. 2010. *The Changing Wealth of Nations: Measuring Sustainable Development in the New Millenium.* Washington, D.C. https://documents.worldbank.org/en/publication/documents-reports/documentdetail/630181468339656734/the-changing-wealth-of-nations-measuring-sustainable-development-in-the-new-millennium.

———. 2022. "Wildlife Conservation Bond Boosts South Africa's Efforts to Protect Black Rhinos and Support Local Communities." Accessed September 2024. https://www.worldbank.org/en/news/press-release/2022/03/23/wildlife-conservation-bond-boosts-south-africa-s-efforts-to-protect-black-rhinos-and-support-local-communities.

Address: 10 Shenton Way, #15-08
MAS Building, Singapore 079117
Website: www.amro-asia.org
Tel: +65 6323 9844
Email: enquiry@amro-asia.org
LinkedIn | Twitter | Facebook | YouTube